國立臺灣大學公共衛生學院全球衛生碩士學位學程

碩士論文

Global Health Program

College of Public Health

National Taiwan University

Master Thesis

比較猴痘在 2022 年之前和 2022 年以後的潛伏期

Comparison of the incubation period of mpox before and
as of 2022

路易吉

Luis Jose Ponce

指導教授：吳亞克博士

Advisor: Andrey Akhmetzhanov, Ph.D.

中華民國 112 年 6 月

June 2023

國立臺灣大學碩士學位論文
口試委員會審定書
National Taiwan University
Verification Letter from the Oral Examination Committee for Master's Students

論文中文題目

2022 年之前和之後猴痘傳播的流行病學參數比較

(Thesis Chinese Title)

論文英文題目

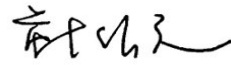Comparison of epidemiological parameters of mpox transmission before and as of 2022

(Thesis English Title)

本論文係　　君（學號 R10853015）在國立臺灣大學全球衛生碩士學位學程完成之碩士學位論文，於民國　　　年　月　日承下列考試委員審查通過及口試及格，特此證明。

This Thesis is written by <u>Luis Jose Ponce (R10853015)</u> studying in the graduate program in the Global Health Program. The author of this thesis is qualified for a master's degree through the verification of the committee.

_____ (指導教授簽名 Advisor Signature)

口試委員 Committee Members:

Acknowledgements

To my parents and to my dear friends
Claire, Eddie, Chloe, Yang-Shen, Danny, Miku, and Arianna,
for their unconditional love and support

To my advisor, the GHP, and Director *Hsien-Ho Lin*,
for providing me with guidance, knowledge, and resources to succeed

And in loving memory of
Charlie

Abstract (Chinese)

引言： Mpox（前稱為猴痘）是一種病毒性疾病，與天花屬於同一家族，其特徵為特殊的皮疹和發燒。Mpox 的症狀從輕微到嚴重不等，可能持續數周，給患者帶來明顯的身體不適和情緒困擾。此外，由於需要專業護理和可能的併發症，Mpox 對醫療系統造成相當的負擔。了解 Mpox 的傳播動力學和關鍵流行病學因素對於制定有效的控制措施，減輕該疾病對公共衛生的影響至關重要。本研究旨在評估 2022 年國際爆發前後 Mpox 病例的傳播動力學，重點是確定平均潛伏期。

方法： 為達到研究目標，我們進行了對 Mpox 傳播事件的系統性回顧，提取了來自不同數據集的暴露和症狀發作日期。使用馬可夫鏈蒙特卡洛抽樣進行潛伏期分佈的估計。採用貝葉斯元分析方法比較並分析本研究和現有同行評審文獻中計算的潛伏期。

結果： 該研究的發現顯示，合併平均潛伏期為 7.80 天，95%可信區間為 6.98 至 8.61 天。值得注意的是，在預 2022 年的水痘疫情和目前的全球疫情之間並未觀察到明顯的流行病學差異。分析還確定了所有後驗暴露至出疹期的 95th、97.5th 和 99th 百分位數分別為 15.7、16.9 和 20.4 天。

結論： 根據研究結果，建議將隔離期限訂為 21 天。值得考慮的是，估計水痘暴露至出疹期間可能提供更多有價值的見解，因為與出疹不同，其他症狀可能不容易被辨認。該研究有助於了解水痘的傳播動態並為公共衛生措施提供有價值的資訊。

關鍵詞： 猴痘、Mpox、貝葉斯統計學、潛伏期、隔離

Abstract (English)
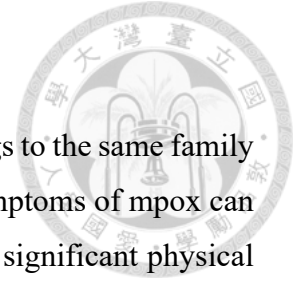
Introduction: Mpox (formerly monkeypox) is a viral disease that belongs to the same family as smallpox and is characterized by a distinctive rash and fever. The symptoms of mpox can range from mild to severe and can persist for several weeks, leading to significant physical discomfort and emotional distress for affected individuals. Additionally, mpox poses a considerable burden on healthcare systems due to the need for specialized care and potential complications. Understanding the transmission dynamics and key epidemiological factors of mpox is crucial for developing effective control measures and reducing the impact of this disease on public health. This study aimed to assess the transmission dynamics of mpox cases before and after the 2022 international outbreak, focusing on determining the average incubation period.

Methods: To achieve the study objective, a systematic review of mpox transmission events was conducted, and exposure and symptom onset dates from different datasets were extracted. Estimations of incubation period distributions were performed using Markov Chain Monte Carlo sampling. A Bayesian meta-analysis approach was employed to compare and analyze incubation periods calculated in this study and in pre-existing peer-reviewed literature.

Results: The findings of the study revealed a pooled mean incubation period of 7.80 days, with a 95% credible interval ranging from 6.98 to 8.61 days. Notably, no distinguishable epidemiological differences were observed between pre-2022 mpox outbreaks and the current global outbreak. The analysis also identified the 95th, 97.5th, and 99th percentiles of all the posterior exposure-to-rash onset draws as 15.7, 16.9, and 20.4 days, respectively.

Conclusions: Based on the study's results, a recommended quarantine period of 21 days is suggested. It is worth considering that estimating the period between mpox exposure and rash onset may provide more informative insights, as other symptoms may not be as easily identifiable as a rash. The study contributes to the understanding of mpox transmission dynamics and provides valuable information for public health measures.

Keywords: monkeypox, mpox, Bayesian statistics, incubation period, quarantine, rash
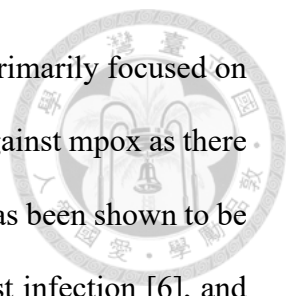
1 Introduction

1.1 History of Mpox Outbreaks

Mpox (formerly known as monkeypox) is a disease caused by the mpox virus, which is a member of the Orthopoxvirus family [1]. The virus is zoonotic, meaning that it originates from an animal reservoir, although the specific species source has yet to be identified. The first human case of mpox was reported in the Democratic Republic of the Congo in 1970, in a 9-month-old boy with an unknown source of transmission [2]. Since then, numerous outbreaks of mpox occurred primarily in Central and West African countries until 2022, when the virus began to spread to several countries in Europe and the Americas. Before 2022, outbreaks were mostly linked to human contact with infected animals or animal products [3], but human-to-human transmission was a driver in many of the outbreaks in 2022-2023.

Initially, mpox outbreaks occurred sporadically with limited human-to-human transmission. For example, from 1970-1986, outbreaks occurred in western and central Africa, with over 400 cases reported. These outbreaks were linked to the hunting and consumption of rodents such as squirrels or some species of monkeys [4]. In 2003, an mpox outbreak occurred in the United States, with 47 confirmed and probable cases reported. Infection from 35 confirmed cases was associated with prairie dogs, and these prairie dogs appeared to have been infected by other rodents [1]. The largest outbreak on record before 2022 occurred in Nigeria in 2017, with 146 suspected cases reported [5]. The outbreak's zoonotic source was unknown and highlighted the need for greater surveillance and preparedness measures. For various reasons, these outbreaks did not spread as widely as mpox is currently spreading.
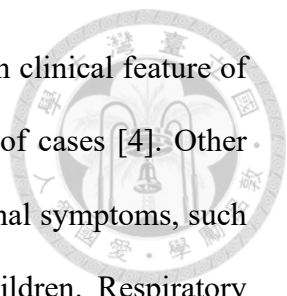
Prior to 2022, efforts to control and prevent mpox outbreaks had primarily focused on early detection and rapid response. Vaccines were not commonly used against mpox as there was no specific vaccine made for the disease, but the smallpox vaccine has been shown to be effective in preventing mpox with evidence of 85% effectiveness against infection [6], and vaccination campaigns were implemented in affected areas [3]. However, the smallpox vaccine was in short supply and had been reserved for high-risk populations, such as healthcare workers and laboratory personnel.

On 23 July 2022, the World Health Organization (WHO) Director-General declared the mpox outbreak as a Public Health Emergency of International Concern (PHEIC) [7]. The WHO has also declared, in November 2022, the shift in name from "monkeypox" to "mpox" due to the stigmatizing and racist language that arose online and in some communities in 2022 following the initial outbreaks. Monkeypox and mpox will be used interchangeably for a year, after which the sole name recognized for the disease will be mpox [8].

1.2 Clinical Characteristics of Mpox
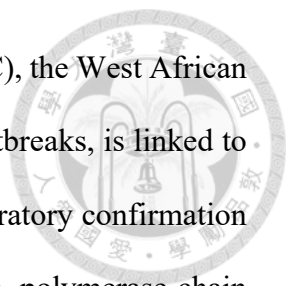
Mpox presents with symptoms similar to those of smallpox, with fever, rash, and lymphadenopathy being the most common clinical manifestations [3]. The disease is usually self-limiting, with the majority of cases resolving within 2-4 weeks. However, severe cases can occur, particularly in immunocompromised individuals, resulting in morbidity and mortality [4]. The rash associated with monkeypox is a distinguishing feature of the disease, and can aid in its clinical diagnosis. The rash typically begins as macules, which progress to papules, vesicles, and pustules before crusting and falling off. The distribution of the rash is variable, but typically involves the face, trunk, and extremities (Fig. 1). The rash can be pruritic, and secondary bacterial infections can occur, particularly in those with severe

disease [3]. In addition to fever and rash, lymphadenopathy is a common clinical feature of mpox, with tender and enlarged lymph nodes occurring in up to 85% of cases [4]. Other common symptoms include headache, myalgia, and chills. Gastrointestinal symptoms, such as nausea, vomiting, and diarrhea, can also occur, particularly in children. Respiratory symptoms, including cough and shortness of breath, have been reported as well [9].

In cases since 2022, clinical symptoms have varied from pre-2022 mpox cases' symptoms, and have been mainly characterized by a prodromal phase with systemic symptoms such as fever, malaise, headache, fatigue, and lymphadenopathy, followed by the appearance of skin lesions or rashes. Lymphadenopathy does not usually occur among chickenpox cases, so swollen lymph nodes can be an important distinguishing factor between the two diseases. In current outbreaks, it has been reported that lesions are firm or rubbery, well-circumscribed, deep-seated, and often develop umbilication, resembling a dot on top of the lesion. The rash may not be disseminated across many body sites and may only appear in a few or a single lesion. Lesions often occur in the genital and anorectal areas or in the mouth, and rectal symptoms such as purulent/bloody stools, rectal pain, or rectal bleeding have been frequently reported [10]. Lesions are often described as painful until the healing phase when they become itchy (crusts). Respiratory symptoms such as sore throat, nasal congestion, or cough may also occur.

Lesions typically develop simultaneously and evolve together on any given part of the body, and they progress through four stages—macular, papular, vesicular, and pustular—before scab formation and desquamation. The evolution of lesions may not always occur in a generalized manner across the body, and they may not appear on palms and soles. The clinical illness usually lasts for 2 to 4 weeks, and the severity of the disease may depend on the initial health of the individual and the route of exposure [10].
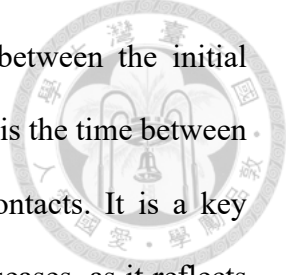
3

According to the Centers for Disease Control and Prevention (CDC), the West African virus genetic group or clade, which is associated with the 2022-2023 outbreaks, is linked to milder disease and fewer deaths than the Congo Basin virus clade. Laboratory confirmation of mpox is typically required to diagnose the disease, with viral culture, polymerase chain reaction (PCR), and serologic testing being used for diagnosis [3]. However, laboratory testing may not be available or accessible in some settings, highlighting the need for greater awareness and surveillance of this disease.

Overall, mpox is a potentially serious disease that can present with a range of clinical manifestations. Early recognition and diagnosis are essential for effective management and control of monkeypox outbreaks.

1.3 Epidemiological Characteristics of Mpox

Epidemiological parameters are essential for understanding and controlling infectious diseases. These parameters help epidemiologists to characterize and quantify the spread of a disease within a population, identify the risk factors, and predict the future course of an outbreak. Without accurate estimates of these parameters, it would be difficult to design and implement effective public health interventions. For example, the basic reproduction number (R_0) is a measure of the number of new infections that can be generated from a single infectious individual in a susceptible population. The effective reproduction number (R_t) is the actual number of new infections generated by each infectious individual at a particular point in time, and takes into account factors such as changes in behavior or interventions like vaccinations. If the effective reproduction number is consistently below 1, it suggests that each infected individual is transmitting the virus to fewer than one other person on average, and the epidemic will eventually die out.

4

Additionally, the incubation period refers to the time interval between the initial infection with a pathogen and the onset of symptoms. The serial interval is the time between symptom onset in an infector and symptom onset in their infected contacts. It is a key parameter for understanding the transmission dynamics of infectious diseases, as it reflects the speed at which the virus is spreading from person to person.

The mean estimated incubation period for mpox has been found to be between 5.6 and 9.1 days, with most cases developing symptoms within 10 days of exposure. The mean serial interval has been estimated to be between 5.6 and 9.5 days, indicating that infected individuals are spreading the virus to others relatively quickly [11]. Monitoring these parameters can help public health officials identify and respond to outbreaks of mpox in a timely manner. However, some factors are hypothesized to affect the length of the incubation period; specifically, the mode of transmission. Mpox exposures are categorized as "complex," referring to invasive modes such as bites, scratches, or piercing with a needle, and "non-invasive," meaning transmission through close contact with an infectious individual.
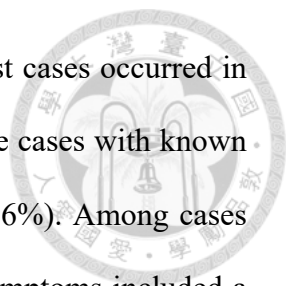
Possible differences in incubation period lengths have been previously studied by Reynolds *et al*. The authors found that for non-invasive exposures, the median incubation period was 13 days, while for complex exposures it was 9 days. Similarly, the median exposure-to-rash onset period was found to be longer for non-invasive exposures, although by a smaller boundary: 15 days for non-invasive and 13 days for complex exposures [12]. In this study, however, all identified human cases were exposed by an animal, and the authors did not include any cases of human-to-human transmission.
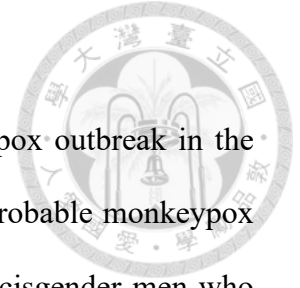
1.4 Current Events of Mpox

Riser *et al*. [13] reported a substantive update on the current mpox outbreak in the United States, as of March 7, 2023. A total of 30,235 confirmed and probable monkeypox cases had been reported in the country by that date, primarily among cisgender men who reported recent sexual contact with another man. Although most of the cases have been self-limited, severe illness and death have been reported. The authors reported that during the period of May 10, 2022, to March 7, 2023, 1.3 deaths per 1,000 cases were mpox-associated: 94.7% of the deaths occurred in cisgender men, and 86.8% occurred in non-Hispanic Black or African American individuals. In this report, the cause of death was determined by the treating health care provider and reported on the death certificate. Deaths were classified as mpox-associated if mpox was listed as a contributing or causal factor, and as non-mpox-associated if mpox was not listed on the death certificate, or if it appeared to be incidental to death. Notably, Black patients had a higher rate of death than of survival, according to the authors. The majority of decedents had sexual or intimate contact with cisgender men in the 3 weeks preceding symptom onset, and some had nonsexual close contact exposures to people with mpox. Homelessness was also prevalent among some of the decedents. Finally, the authors also found that HIV infection was more prevalent among decedents than survivors.

Outside of the United States, as of April 4, 2023, there were a total of 25,874 cases of mpox identified in 45 countries throughout the European region. Within the four weeks prior, there were 28 cases identified in seven countries. The data were reported to the European Centre for Disease Prevention and Control (ECDC) and the World Health Organization (WHO) Regional Office for Europe through the European Surveillance System (TESSy). Out of the cases reported, most were confirmed through laboratory testing [14].

The earliest reported onset of symptoms was April 17, 2022. Most cases occurred in males (98%) aged between 31 and 40 years (39%). The majority of male cases with known sexual orientation identified as men who have sex with men (MSM) (96%). Among cases with known HIV status, 38% were HIV-positive. The most common symptoms included a rash (96%) and systemic symptoms such as fever, fatigue, muscle pain, chills, or headache (68%). Out of the 16,027 cases with reported symptoms, 783 (6%) required hospitalization, and 271 cases required clinical care. Unfortunately, six cases resulted in death, and eight cases required intensive care unit (ICU) admission [11].

Although not as prevalent as Europe and the Americas, mpox outbreaks have also affected several countries in Asia. The first location in the continent to report a confirmed case was Israel on May 20, 2022 [15]. Since then, very few cases have been reported in countries across West, South, and Southeast, Asian countries such as India, Bangladesh, Thailand, and Singapore [16]. However, in East Asian countries, the number of mpox cases has been gradually spreading at higher rates. For example, in Japan, confirmed cases have surpassed 100, and Taiwan's cases have also been increasing since the spring of 2023 [17].

To prevent mpox deaths, public health actions should include integrated testing, diagnosis, and early treatment for mpox and HIV, as well as ensuring equitable access to both mpox and HIV prevention and treatment. The report also highlights the importance of targeted interventions to address health disparities among vulnerable populations, such as Black individuals and those experiencing homelessness. The findings of this report emphasize the ongoing need for vigilant monitoring, response, and communication to address the current mpox outbreak in the United States and around the world.
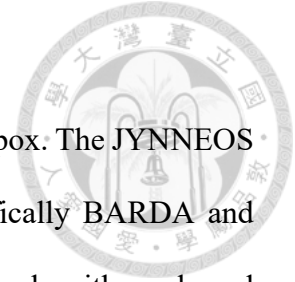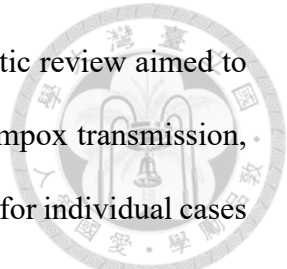
1.5 Public Health Responses to Mpox

Vaccine developers quickly created an effective vaccine against mpox. The JYNNEOS vaccine was created in partnership with the U.S. Government (specifically BARDA and BioShield) to provide protection against smallpox, including for individuals with weakened immune systems or who are at high risk for adverse reactions to traditional smallpox vaccines. Research published in Nature Medicine found that a single dose of the Modified Vaccinia Ankara-Bavarian Nordic vaccine (which is used in the JYNNEOS vaccine) can protect against mpox, with the latter study estimating an adjusted vaccine effectiveness of 86% for males [18].

In countries where the mpox vaccine is available, this has been the main method of intervention against the spread of the virus. However, less fortunate countries have had multiple different responses. In May and June 2022, several countries issued warnings and took measures to prevent the spread of mpox, a disease caused by the monkeypox virus. For example, in India, the Union Health Ministry directed the National Centre for Disease Control and the ICMR to monitor the situation closely and instructed airport and port health officers to isolate and send samples to the National Institute of Virology of any sick passenger with a travel history to infected countries [19]. Elsewhere, the Saudi Ministry of Health stated that they were ready to monitor and investigate cases of mpox [20].

1.6 Research Objectives

Since the start of mpox outbreaks in the Global North, some studies have estimated the mean incubation period. However, none have attempted to compare the observed incubation period to the data before the 2022 outbreaks. I aimed to systematically review mpox transmission literature before 2022 to gather and analyze all available data on this specific

8

topic that has not been previously gathered or synthesized. This systematic review aimed to provide a comprehensive and structured approach to collecting data on mpox transmission, with a specific focus on the dates of disease exposure and symptom onset for individual cases prior to the 2022 outbreaks. By conducting a systematic review, this study aimed to provide a more complete and accurate understanding of the epidemiology and public health implications of mpox transmission, and to provide a foundation for further research and potential intervention.

Through a meta-analysis of the resulting data from the systematic review and several other datasets containing estimated incubation periods and corresponding 95% credible intervals (CrI), I aimed to compare the available estimated incubation periods of mpox through meta-analyses to then compare the results and investigate any significant difference in estimates, if present.

Finally, I strive to use my results to inform public policy with epidemiological parameter estimates from pre-2022 data especially, which may work as a proxy for the current global mpox outbreaks. For example, current public health officials are debating details of the duration of quarantine for mpox confirmed cases, and whether quarantine should be implemented for close contacts of confirmed cases.
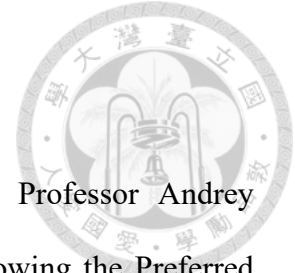
2 Methods

2.1 Systematic Review and Meta-Analysis

To ensure a thorough and meticulous identification of data, Professor Andrey Akhmetzhanov and I began with a systematic search and review following the Preferred Reporting Items for Systematic Reviews and Meta-Analyses (PRISMA) protocol [21]. This review was not registered. This study was exempt from ethics review because all data sources and were from previously published literature.
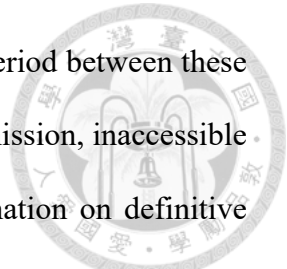
2.1.1 Search Strategy

We began our search by using the key words "monkeypox" AND ("symptoms" OR "onset" OR "exposure") in the PubMed electronic database to identify publications. In addition, one other record was found through the WHO Disease Outbreak News website. We screened the reports independently by compiling all of them into a shared file, and collected only those data with dates of exposure and symptom onset for individual definitive cases. When these dates were unknown or unclear, we did not include the data, and if a range of dates for exposure or symptom onset was known, even if the exact dates were not, we included such publications.

Additionally, while we searched for similar data on incubation period for 2022 and 2023 mpox outbreaks, a systematic search was not possible due to the ongoing nature of the outbreak and the real-time publication of related studies. Instead, we relied on mpox updates to identify relevant studies and extract data on the dates of disease exposure and symptom onset to estimate the mean incubation period and include these data in my meta-analysis.

2.1.2 Inclusion and Exclusion Criteria

First, inclusion criteria for selected pre-2022 studies were that information of individual mpox cases before 2022 were detailed in the text, and that at least one individual

case had the dates of mpox exposure and symptom onset listed, or the period between these two dates listed. Exclusion criteria were: no information on mpox transmission, inaccessible publications, no information on individual mpox cases, and no information on definitive exposure. Inaccessible studies were those that lacked full electronic versions. Studies with overlapping data (i.e., the same individual cases) were included only if they provided additional information about the desired data.

Next, for 2022 and 2023 studies' inclusion in the meta-analysis, since, in addition to the mean incubation period, a standard error value is also necessary, only peer-reviewed studies with both mean incubation period estimates and their 95% CrI were selected. In addition to the pre-2022 mpox data, we were able to find and use four more datasets. One of these datasets was collected by Viedma-Martinez et al. [22], who collected detailed data on mpox cases' dates of exposure and symptom onset that occurred in a tattoo parlor in Cadiz, Spain. However, the authors did not calculate any incubation period estimates, so the estimates were performed in this study. Next was the data used by Miura et al. [23]. Although Miura et al. had their own incubation period estimates, the statistical methods were re-evaluated and the data were re-analyzed in the present study. Then, the largest available data set came from a series of cases in the whole country of Spain, collected by Tarin-Vicente et al., who did not offer their own Bayesian estimates of the mean incubation period [24]. Finally, a dataset consisting mostly of U.S. mpox cases, collected by Madewell et al. [25], was included in the meta-analysis conducted in this study.

2.1.3 Outcome Measures and Study Selection
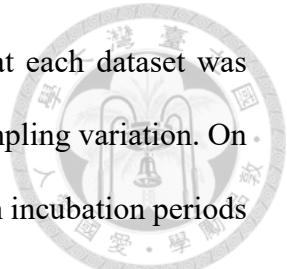
The outcome variable within each dataset was the mean estimate of the incubation period, specifically the exposure-to-symptom onset period. It was measured for all cases

within each dataset with information on what day they were exposed to mpox and what day their symptoms began.

For the pre-2022 mpox publications, search results were screened first through titles and abstracts. In this screening stage, publications without full electronic texts available and irrelevant studies were removed. The full texts of the remaining studies were examined and, in the next screening stage, those without the required data—definitive exposure and individual case information—were removed during the screening process. For the current mpox outbreak studies, new studies were included in the meta-analysis as their data became available. Then, data extraction was conducted for the remaining articles that made it through the screening process. When available, we aimed to collect data about studies' author names, publication date, and for each individual case ID, sex, age, country of origin, disease exposure and symptom onset date, rash onset date, list of symptoms, testing date, disease confirmation date, source of infection, transmission method, and disease status (i.e., confirmed, probable, or suspected).

2.1.4 Meta-Analysis

After completion of data extraction and synthesis, two types of meta-analysis were applied to selected studies: a "pooled" model and a "hierarchical" or "partially pooled" model, which represent a frequentist and a Bayesian approach to conducting meta-analyses. The inclusion criteria for the meta-analysis involved the presence of an estimated mean exposure-to-symptom onset period and its corresponding 95% CrI. Additionally, the exposure-to-symptom onset periods and credible intervals calculated in the present study were included in the meta-analysis.

The more classic frequentist meta-analysis approach assumes that each dataset was sampled from the same model, which ignores all variation other than sampling variation. On the other hand, a Bayesian meta-analysis approach assumes that the mean incubation periods (i.e., effect sizes) are random variables and can vary between studies; it accounts for heterogeneity between studies, which is crucial to consider. Different datasets contain differences in study populations, diagnostic methods, and other factors. Heterogeneity accounts for the variation in these factors and results in outputs that reflect the uncertainty across different datasets, which may consequently lead to a more accurate estimation of the average incubation period, particularly when the number of included studies is small. Bayesian meta-analysis produces a posterior distribution for the mean incubation period, which allows for the calculation of the exact probability that the mean is smaller or larger than a specified value [26].

The pooled model assumes that for a set of independent studies, $i = 1, \ldots, k$, and observed mean incubation periods for each study, y_i, then θ_i denotes the corresponding "true"/pooled incubation period. This model also assumes random effects, meaning that the true mean incubation periods are normally distributed with mean μ and variance τ^2 representing the heterogeneity between data sets. Random effects are used to account for variability between different studies' incubation period estimates, and are especially useful when the number of studies or data sets is relatively small compared to the total sample size. The true incubation period in this meta-analysis approach is estimated by (1).

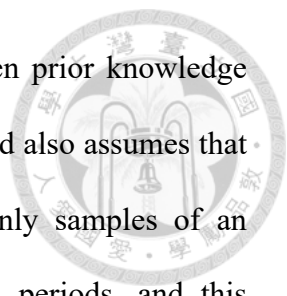$$\theta_i \sim N(\text{mean} = \mu, \text{variance} = \tau^2) \tag{1}$$

Each incubation period is assumed to have measures of uncertainty associated with the observed mean incubation periods, denoted as the standard errors (SE) calculated by (2)

$$SE_i = (\text{Upper CrI } y_i - \text{Lower CrI } y_i)/(2 \times 1.96) \qquad (2)$$

In (2), the upper and lower CrI are the 95% upper and lower bounds of the mean incubation period for each dataset. The value 1.96 corresponds to the critical value for a 95% confidence level in a normal distribution. Therefore, this model accounts for both the within-study variability and between-study heterogeneity.

For this meta-analysis, the DerSimonian and Laird (DL) method was used, which is a statistical approach commonly used in meta-analysis to estimate the pooled effect size or mean effect across multiple independent studies. It is particularly suitable when there is an unknown level of heterogeneity, or variation, among the studies' estimated parameters [27]. In addition to the DL method, the I^2 statistic is commonly used in meta-analysis to assess the degree of heterogeneity among the studies included in the analysis. Conceptually, I^2 represents the proportion of total variation in the estimated effects that is due to heterogeneity rather than chance. The I^2 statistic ranges from 0% to 100%, with higher values indicating greater heterogeneity. It provides insights into the consistency or inconsistency of the estimated parameters across studies. A value of 0% suggests no observed heterogeneity, while higher values indicate increasing levels of heterogeneity. In the context of this study, the I^2 statistic helps evaluate the variability in incubation period estimates among the different datasets and provides information about the extent to which the true incubation period may vary across studies. In addition, the Q statistic in meta-analyses complements the I^2 statistic by quantifying the statistical significance of heterogeneity among the included studies. It assesses whether the observed variation in incubation periods is greater than what would be expected by chance, helping to determine if the differences in the estimated parameters across studies are statistically significant.

In contrast, the partially pooled/hierarchical model uses the given prior knowledge about mpox's mean incubation period and its respective variance, σ^2, and also assumes that the true mean incubation periods of mpox from each dataset are only samples of an overarching Normal population distribution of true mean incubation periods, and this distribution has mean μ and variance τ^2, which represents the between-study heterogeneity. The observed mean incubation period, denoted as $\hat{\theta}_k$, is assumed to deviate from the true mean incubation period, θ_k, due to some sampling error. Therefore, the true mean incubation period—i.e., the partially pooled mean—is estimated by

$$\hat{\theta}_k \sim N(\text{mean} = \mu, \text{variance} = \sigma_k^2 + \tau^2) \tag{3}$$

Where $N(\mu, \sigma_k^2 + \tau^2)$ indicates the normal distribution. Weakly informative priors were used, so as to not influence the posterior values. This meta-analysis model provides a full posterior distribution, whereas the former meta-analysis model focuses instead on obtaining the best true parameter point estimates and their variability.

2.2 Data Descriptions and Preparation for Analysis
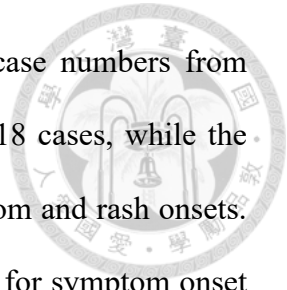
To meet the inclusion criteria, each case found in the literature was required to have information on both the date of symptom onset and an exposure date, whether it was provided as a left or right boundary. The inclusion of left and right boundaries was necessary due to potential uncertainty in recall and interview data, which can affect the accuracy of determining the exact days of exposure or symptom onset. Moreover, the precise timing of exposure or symptom onset is important for estimating the incubation period. In some cases, the right boundary of the exposure date was missing. However, it is clear that exposure must have occurred no later than the same day as symptom onset. Therefore, any missing right boundaries of exposure dates were set to be equal to the right boundary of the symptom onset

date. On the other hand, there was generally less uncertainty regarding the symptom onset date, as it is typically easier to determine when symptoms began. The right boundary of symptom onset was set as the left boundary plus one day to account for possible variations in the time of day when symptoms may have started.
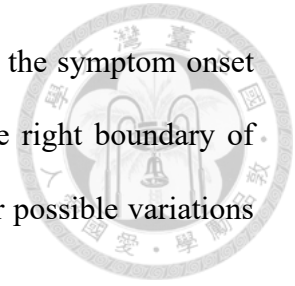
A total of 42 unique mpox transmission cases from sources before 2022 were included in the analysis for estimating the exposure-to-symptom onset period. Of those 42 cases, there was a total of 38 observed cases and 4 censored cases, which were used for further analysis and estimation. Similar data preparation techniques were applied to estimate the mean exposure-to-rash onset period. However, collecting data on rash onset is less common during case interviews, resulting in a smaller number of cases. Specifically, the observed data for rash onset in the synthesized pre-2022 dataset consisted of only 20 cases, including 4 censored cases, indicating a reduced sample size for this particular analysis.

For the remaining datasets utilized in the statistical analyses of this study, the calculation of left and right boundaries for exposure and onset dates followed a similar approach if they were not already provided in the raw data. Specifically, for the Netherlands dataset by Miura *et al*. [23], where the exact time of exposure was unknown but the date was available, the left boundary was assigned as the recorded date, while the right boundary was set as the recorded exposure date plus one day. Regarding the symptom onset date, its precise information allowed for the determination of the left boundary, while the right boundary was calculated as the recorded symptom onset date plus one day. Likewise, in the case of the tattoo parlor outbreak dataset reported by Viedma-Martinez *et al*. [22], only the dates of exposure and symptom onset were available without precise times. To account for potential variability of infection or symptom onset within a day, one day was added to the left boundaries of both the exposure and symptom onset dates.

16

The data sets used for the meta-analyses consisted of various case numbers from different sources. Specifically, the dataset from Miura *et al*. included 18 cases, while the dataset from Viedma-Martinez *et al*. contained 21 cases for both symptom and rash onsets. Additionally, the dataset from Tarin-Vicente *et al*. comprised 144 cases for symptom onset and 143 cases for rash onset, and the dataset from Madewell *et al*. consisted of 36 cases for symptom and rash onsets [22]–[25]. These diverse datasets contributed to a comprehensive analysis of mpox transmission dynamics and provided valuable insights into the exposure-to-symptom onset period and exposure-to-rash onset period of the disease. Therefore, the total number of individual samples for the exposure-to-symptom onset period estimations was $n = 260$ and for the exposure-to-rash onset estimations was $n = 220$.

2.3 Statistical Analyses

Initially, exposure-to-symptom onset period distributions of mpox were estimated using Markov Chain Monte Carlo (MCMC) sampling techniques for each available dataset. Subsequently, a meta-analysis was conducted by pooling the exposure-to-symptom onset periods reported in the literature, along with the estimated values obtained from the present study's analysis, and employing a Bayesian hierarchical/partial pooling model. Furthermore, a secondary analysis was performed by examining the mean length of the interval between exposure and rash onset. Similarly, a Bayesian meta-analysis was conducted for studies with mean exposure-to-rash onset estimates and 95% credible intervals. All probability distribution models were created using CmdStan version 2.31.0 [28]. The remaining statistical analyses were conducted using R version 4.2.3 [29].

2.3.1 Bayesian Statistics and Markov Chain Monte Carlo Sampling

Bayesian statistics is a branch of statistics that uses Bayes' theorem to update the probability of a hypothesis as new evidence becomes available. In contrast to classical statistics, Bayesian statistics provides a framework for incorporating prior knowledge into statistical analyses. Bayesian methods have become increasingly popular in epidemiology due to the flexibility they offer in incorporating prior knowledge about the disease and the population under study. When applied to epidemiology, Bayesian statistics can be used to estimate parameters of interest such as the incubation period of a disease. By incorporating prior knowledge, Bayesian methods can provide more accurate estimates and credible intervals for the parameter of interest. Additionally, Bayesian methods can be used to estimate the probability of a certain outcome, such as the probability of an outbreak occurring, given certain assumptions and data.

One commonly used Bayesian method is Markov Chain Monte Carlo, which allows for the simulation of posterior distributions of parameters. MCMC has been used in a variety of epidemiological applications, such as estimating the incubation period of COVID-19 and estimating the effectiveness of vaccination programs [30], [31]. Bayesian statistics offers a powerful framework for incorporating prior knowledge into epidemiological analyses, allowing for more accurate estimates of disease parameters and probabilities. MCMC is a commonly used Bayesian method that enables the simulation of posterior distributions and has been applied to a variety of epidemiological problems.

Applied to the present study, since there is prior knowledge about mpox and its incubation period, I combined the prior knowledge with new data to update parameter estimates and make inferences. This method is particularly useful when the sample size is small or the data are incomplete, as is the case for the most datasets analyzed in this study.
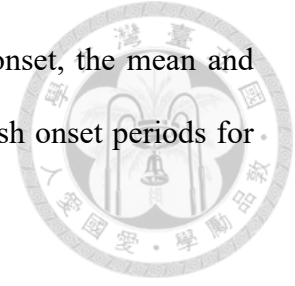
By using the data about the dates of disease exposure and symptom onset, the mean and distributions of exposure-to-symptom onset periods and exposure-to-rash onset periods for mpox were estimated.

2.3.2 Probability Distributions

Log-normal, Weibull, and gamma distribution models were employed to estimate the mean exposure-to-symptom onset period and mean standard deviation for three distinct datasets of monkeypox. Later, these same models were used to estimate the mean length between exposure and onset of either a rash or other symptoms. All considered distributions are defined only on positive values.

2.3.2.1 Weibull Distribution

The Weibull distribution is a flexible probability distribution that can be used to model a wide range of data types. It is characterized by two parameters, shape (k) and scale (λ), and its probability density function (PDF) has a shape that can be either increasing, decreasing, or constant over time (4). The PDF represents the probability of obtaining a specific value of a random variable in a given distribution. It is used to calculate the mean, variance, and other statistics of a distribution.

$$\text{For } x \geq 0, \ f(x) = \frac{k}{\lambda}\left(\frac{x}{\lambda}\right)^{k-1} e^{-(x/\lambda)^k} \tag{4}$$

The mean and standard deviation (SD) of the Weibull distribution are given by (5) and (6), respectively.

$$\text{mean} = \lambda \Gamma(1 + {}^{1}/_{k}) \tag{5}$$

$$SD = \lambda \sqrt{\Gamma\left(1 + {}^{2}/_{k}\right) - \left(\Gamma\left(1 + {}^{1}/_{k}\right)\right)^{2}} \tag{6}$$
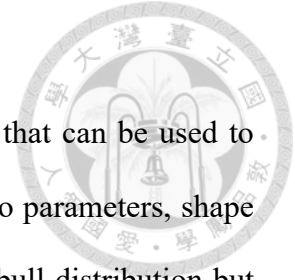
2.3.2.2 Gamma Distribution

The Gamma distribution is a continuous probability distribution that can be used to model a wide range of real-world phenomena. It is characterized by two parameters, shape (α) and rate (β), and its PDF (7) has a shape that is similar to the Weibull distribution but with a longer tail. The shape parameter (α) controls the shape of the Gamma distribution and can be used to model data with different levels of skewness.

$$f(x) = \frac{\beta^\alpha}{\Gamma(\alpha)} x^{\alpha-1} e^{-\beta x} \tag{7}$$

The mean of the gamma distribution is given by (8)

$$mean = \frac{\alpha}{\beta} \tag{8}$$

and its standard deviation by (9).

$$SD = \frac{\sqrt{\alpha}}{\beta} \tag{9}$$

2.3.2.3 Log-Normal Distribution

The log-normal distribution is a continuous probability distribution that can be used to model data that is non-negative and skewed to the right. It is characterized by two parameters, location (μ) and scale (σ), and its PDF (10) has a shape that is similar to the normal distribution but skewed to the right. The scale parameter (σ) controls the spread of the distribution, while the location parameter (μ) shifts the distribution to the left or right.

$$f(x) = \frac{1}{x\sigma\sqrt{2\pi}} e^{\left(-\frac{(\ln x - \mu)^2}{2\sigma^2}\right)} \tag{10}$$

The mean and standard deviation for the log-normal distribution are given by the following equations, respectively.

$$mean = e^{\mu + \sigma^2/2} \tag{11}$$

$$SD = \sqrt{e^{\sigma^2 - 1}} e^{\mu + \sigma^2/2} \tag{12}$$

2.3.3 Fitting the Data and Exposure-to-symptom onset Period Estimations

The study involved multiple datasets, each containing information on exposure dates, symptom onset dates, and sometimes rash onset dates. Pre-existing boundaries were utilized for datasets with available left and right boundaries, while appropriate values were assigned to datasets without provided boundaries to ensure accurate estimation. Censored data was handled by assigning it a weakly informative prior distribution given by (13). Then, data lists were constructed for each dataset and descriptively named, including the number of observations (N), exposure dates' left boundaries (EL), symptom or rash onset dates' left boundaries (OL), and corresponding right boundaries of these dates (ER and OR) when available. For situations where data were missing, the data lists included censored and observed counterparts, such as censored case observations (N_{cens}), complete case observations (N_{obs}), censored left boundary exposure dates (EL_{cens}), and observed ones (EL_{obs}).

$$EL_{cens} \sim \text{Exponential}(\text{rate} = 0.01) \tag{13}$$

To incorporate the data into the Bayesian modeling framework, the model code in CmdStan included a "data" block specifying the variables' properties, such as N as an integer and EL, OL, and other relevant vectors. In the "transformed data" block, additional transformations were performed on the data, specifically incrementing the onset start times (OL) and exposure start times (EL) by one unit to represent the right boundaries (OR, ER), where applicable. Furthermore, parameters e and o were sampled from EL, ER, OL, and OR, defined in (14) and (15). In these equations, e_{raw} and o_{raw} generate random numbers between 0 and 1 following a uniform distribution, Uniform(0, 1), representing different fractions of the day. Overall, by organizing the data into the appropriate format and performing necessary

<div align="center">21</div>

transformations, the dataset was prepared for further analysis using the specified model code (Appendix).

$$e = EL + (ER - EL) \times e_{raw} \qquad (14)$$

$$o = OL + (OR - OL) \times o_{raw} \qquad (15)$$
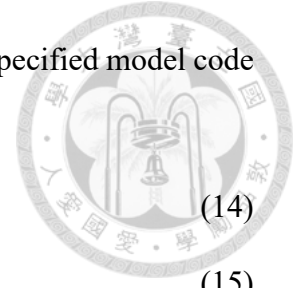
This study also corrected for right-truncated data when the truncation date was known and was not already corrected. Right truncation refers to the fact that at the time of data collection, some cases had not yet experienced symptom or rash onset, which is a common scenario during ongoing epidemic events, where data are collected in real-time as the epidemic unfolds. If these cases are not accounted for, it can introduce bias and affect the estimation of the exposure-to-symptom onset period and exposure-to-rash onset lengths. By considering right truncation, the parameters calculated in this study were more accurately estimated by including cases that are still within the latent period but will eventually develop symptoms. Failure to account for right truncation may lead to underestimation of these epidemiological parameters, as cases with longer incubation periods may not have been captured in the analysis. Formally, it may be written as (17), explained below.

Each of the three distribution models utilized in this study produced estimates for the mean exposure-to-symptom onset period and its SD. Additionally, respective 95% credible intervals were calculated for each mean and SD.

2.3.4 Model Assessment and Selection Through Likelihood Functions

After composing all the models for each analyzed dataset and fitting the corresponding data to each, I assessed and ranked the performance of the models to determine which distribution shape best fits the data. To apply model comparisons, the log-likelihoods, which

22
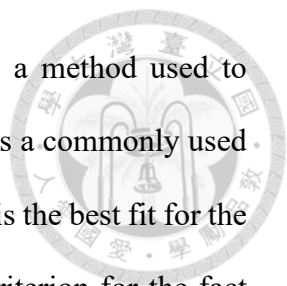
represent functions that measure the goodness of fit of a probability distribution model to the fitted observed data were calculated. It quantifies the logarithmic likelihood of observing the data, given the specific parameters used in each model. The log-likelihood is conventionally used instead of the likelihood itself for computational convenience and because it simplifies calculations involving probabilities. Conceptually, a higher log-likelihood indicates a better fit of the data to that model.

As applied in this study, the logarithm of the likelihood of observing the given exposure-to-symptom onset period under the assumption that it follows a specific distribution, was calculated for each of the three distribution models. For individual data points denoted as x_i, the likelihood functions of the Weibull, gamma, and log-normal probability distributions are given by (16) where $f(o_i - e_i)$ represents the PDF of the exposure-to-symptom onset period or exposure-to-rash onset period and parameters 1 and 2 represent the corresponding shape or rate and scale parameters. Then, the logarithm of each likelihood was calculated using the corresponding built-in "lpdf" function in CmdStan.

$$L(o - e|param\ 1, param\ 2) = \prod_{i=1}^{n} f(o_i - e_i \mid param\ 1, param\ 2)$$

(16)

For the inclusion of right truncation, the likelihood function was altered, this time including the cumulative distribution function (CDF) of each considered distribution, represented as $F(o_i - e_i)$ in (17). The CDF represents the integral or area under the curve of the PDF [32].

$$L(o - e|param\ 1, param\ 2) = \prod_{i=1}^{n} \frac{f(o_i - e_i \mid param\ 1, param\ 2)}{F(o_i - e_i \mid param\ 1, param\ 2)}$$

(17)

23

Leave-one-out cross-validation information criterion (LOOIC) is a method used to evaluate the accuracy of model selection in Bayesian stat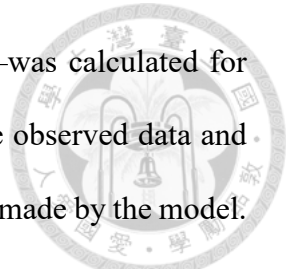istics. LOOIC is a commonly used measure of model fit, and it helps in determining which statistical model is the best fit for the data under investigation. LOOIC specifically adjusts the information criterion for the fact that the model is estimated from the same data it is being used to predict. This is done by removing one observation at a time from the data set and recalculating the likelihood based on the remaining data. This process is repeated for each observation, and the resulting likelihoods are then used to calculate LOOIC.

This method has been shown to be a reliable and accurate method for model selection in many applications, including epidemiological studies. LOOIC is a preferred measure over traditional methods such as Widely acceptable information criterion (or Watanabe-Akaike information criterion) (WAIC) and Bayesian information criterion (BIC) for model selection due to its efficiency and reliability, according to Vehtari *et al*. [33]. Unlike WAIC and BIC, LOOIC does not suffer from biases introduced by the fixed number of parameters and has better consistency and robustness properties. LOOIC also allows for comparison of non-nested models—i.e., models that cannot be directly ranked or compared by traditional methods—and can be used to estimate the expected logarithmic predictive density for new data. Additionally, LOOIC is considered better than WAIC in some cases because it provides more accurate approximations of the expected logarithmic pointwise predictive density, especially in situations with a small sample size or when there is overdispersion in the data. LOOIC is also more reliable and robust for model selection than WAIC, as it is less sensitive to small changes in the model or data and less likely to produce overconfident inferences or overfitting of the model [33].

24

Afterwards, the deviance—which is -2 times the log-likelihood—was calculated for each model. The deviance assesses the goodness of fit of a model to the observed data and quantifies the discrepancy between the observed data and the predictions made by the model. It is derived from the likelihood function, and a lower deviance value indicates a better fit of the model to the data, suggesting that the model can explain a larger proportion of the observed variability. Rather than reporting LOOIC estimates, which are less intuitive, the deviance for each model was reported in this study for ease of interpretation. Generally, if the difference in deviance between models is less than two (ΔDeviance < 2), then it means that one model does not provide a significantly better fit to the data compared to the other.

2.3.5 Exposure-to-Rash or Symptom Onset Period

Similar to exposure-to-symptom onset period estimations, for data sets where the dates of rash onset were available, I estimated the mean period from mpox exposure to rash onset. The time interval between exposure and rash onset is an essential piece of information in identifying cases of mpox infection. This is particularly significant as non-rash symptoms of the disease can be easily confused with those of other illnesses. A rash, on the other hand, is a clear and mostly unambiguous symptom of mpox. Therefore, understanding the exposure-to-rash onset period can provide valuable information about the progression of the disease and the likelihood of its spread.

Moreover, it is crucial to investigate whether mpox transmission commonly occurs before symptom onset or after initial symptoms onset but before the appearance of a rash. This is important because individuals infected with mpox may transmit the virus to others before exhibiting any symptoms, making it difficult to identify and isolate cases promptly.

Consequently, examining the period of infectiousness before the onset of symptoms or rash can aid in developing effective control strategies for the disease.

3 Results

3.1 PRISMA Systematic Review

Our pre-2022 mpox transmission literature search yielded a total of 332 records, including 331 from PubMed and 1 from a WHO report. To begin the screening process of the review, we carefully assessed the title and abstract of each record and excluded 236 that were irrelevant to mpox transmission. The remaining 92 records were further assessed for eligibility by reviewing the full text, resulting in the exclusion of 55 records that did not provide information on individual mpox cases and 18 that lacked information on definitive exposure. Of the remaining sources, we also identified 4 articles that contained duplicated data from previously assessed sources, but were included because they provided additional information. Ultimately, we used a total of 19 articles to extract comprehensive data on mpox transmission, including case identification and dates of exposure and symptom onset, necessary for incubation period estimations that I aimed to do (Fig. 2) [34]–[52].

After completing the systematic search and review for pre-2022 mpox transmission data, a similar search and review was conducted to identify studies on incubation period estimates from global mpox outbreaks that started in 2022 and onwards. Since the publication of peer-reviewed articles happened in real-time as we were conducting the research, we used a different literature search approach. We identified relevant literature as they were published, then found more relevant studies from the citations of the initial articles. We identified a total of 35 peer-reviewed studies on mpox incubation period estimates.

Upon screening these 35 studies, 28 of them were irrelevant to the research question because they did not contain the incubation period data required for inclusion. After carefully assessing the remaining 7 studies by reviewing the full text of each article, 2 articles were

excluded because they only provided the median incubation period and not the mean incubation period. Ultimately, there were 5 studies that contained the relevant data for the present study [22]–[25], [53]. With these data, I proceeded to analyze and synthesize the incubation period estimates from these studies (Fig. 3).

After conducting the incubation period literature search and extracting relevant data, I moved on to visualizing my findings in a forest plot. I included both median and mean exposure-to-symptom onset period estimates in this plot, as well as non-peer-reviewed estimates for the sake of thoroughness. A non-peer-reviewed estimate is distinguished in the forest plot, and the estimates calculated in this study are also represented on the plot (Fig. 4A), and summarized in Table 1.

3.2 Estimated Mean Exposure-to-Symptom Onset Periods and Model Assessments

Among all of the currently available mpox exposure-to-symptom onset period estimates, the present study focused on studies reporting the distribution of exposure-to-symptom onset periods along with the mean and 95% CrI of that distribution for the hierarchical meta-analyses. Then, the present study created IP distributions for datasets where it has not been done before or where estimates can be further improved.

3.2.1 Pre-2022 Data

To account for the time variation in a day, the right boundaries of onset dates were assigned to be equal to the left boundary date plus one day. For example, if exposure was recorded as occurring on January 1st and was the first in its respective outbreak, then it would be assigned as day 1, and symptom onset on January 9th would be assigned as day 9. The missing left boundary exposure dates were estimated using a weakly informative prior and using the cases where data were complete to assign values to the missing exposure dates.

Mean exposure-to-symptom onset period estimates and the standard deviation of the exposure-to-symptom onset period are reported in Table 3 along with their corresponding 95% credible intervals.

Moving forward, the log-likelihood for each distribution model was generated. Using the calculated log-likelihood values, LOOIC was performed to evaluate the goodness of fit of each model. Additionally, the deviance of each model was calculated also using the log-likelihoods, and these values were reported in Table 4. For this pre-2022 dataset, none of the distribution models was a significantly better fit than the other.

3.2.2 Tarin-Vicente *et al*. Data

A study conducted by Tarin-Vicente *et al*. aimed to investigate the clinical and virological characteristics of human mpox cases in Spain reported in May and June 2022. They conducted a multicenter, prospective, observational cohort study in three sexual health clinics in Madrid and Barcelona, Spain, and enrolled all consecutive patients with laboratory-confirmed mpox from May 11 to June 29, 2022. The authors collected participant data by conducting interviews using a standard case report form and offered lesion, anal, and oropharynx swabs for PCR testing [24]. In addition to collecting data on date of infection and symptom onset, they also collected data on rash onset dates. The date of right truncation is also known and was accounted for in the statistical analyses.

Mean exposure-to-symptom onset period estimates adjusted for right truncation and standard deviations for all distribution models are summarized in Table 3. The deviances for the Weibull, log-normal, and gamma distribution models summarized in Table 3 show that the gamma distribution model had the lowest value, meaning it was the best fit.

29
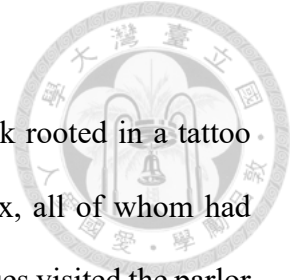
3.2.3 Viedma-Martinez *et al*. Data

Identification of case transmission data of mpox from an outbreak rooted in a tattoo parlor in Cadiz, Spain resulted in 21 confirmed reported cases of mpox, all of whom had visited the tattoo parlor around the same couple of weeks. Most of the cases visited the parlor to get a piercing except for one, who got a tattoo only [22]. To extract and synthesize data for the dates of exposure and dates of symptom onset, I retrieved all available information from the relevant sources. While I could retrieve the date, I could not retrieve the exact time. Therefore, the dates I identified were marked as the left ends of exposure and symptom onset.

Calculated estimates for this dataset are also summarized in Table 3. After comparison of the deviance values for each probability distribution model, the log-normal distribution model was selected as the best fit (Table 3).

3.2.4 Miura *et al*. Data

Adding to a study published in 2022 by Miura *et al*. [23], I used their data for my own analyses to estimate the exposure-to-symptom onset period. These data were collected from an outbreak of mpox in the Netherlands and had exact dates of exposure for 13 out of 18 cases, and the exact dates of symptom onset for all cases. Where exposure date was uncertain, a range of dates was available, with a left boundary and a right boundary [23]. The purpose of this step was to either validate or revise the estimates first reported by the authors.

Yielded exposure-to-symptom onset period estimates in this study were similar but not identical to Miura *et al*.'s estimates. All mean and standard deviation estimates are again summarized in Table 3. To assess and select the distribution that best fit the data, the LOOIC method was applied and the deviance was calculated for each model. The deviances revealed that the best-fit model was the log-normal distribution (Table 4).

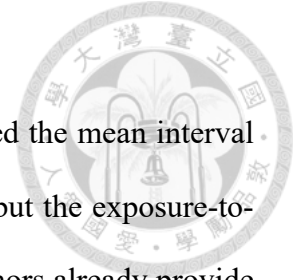### 3.3 Estimated Exposure-to-Rash Onset Period and Model Assessments

In addition to exposure and symptom onset data for exposure-to-symptom onset period estimations, certain datasets also contained rash onset information, which allowed for the estimation of the exposure-to-rash onset period. As rashes are a more distinctive symptom of mpox, estimating this period may provide more insight into appropriate contact tracing and quarantine measures to contain disease transmission. Mean estimates of this parameter along with their respective 95% CrI are visualized in Fig. 4B and corresponding values are summarized on Table 2.

3.3.1 Pre-2022 Data

Consistent with previous estimates, I employed a left-hand and right-hand boundary for the exposure date and rash onset date. Specifically, the right-hand boundary was defined as the left-hand boundary plus one day. To address the variability and uncertainty regarding the precise time of exposure within a given day, I introduced a uniformly distributed parameter ranging from 0 to 1. Then, the best-fit model was selected through LOOIC methods. The mean exposure-to-rash onset periods and standard deviations and deviances are summarized in Table 5 and Table 6. For this parameter involving rash onset, there was no significantly best-fit model.

3.3.2 Tarin-Vicente *et al*. Data

Similar to exposure-to-symptom onset period estimates, right truncation was accounted for here, as the date of truncation was known. For this study, the Weibull distribution model was also found to be the best fit. The best-fit model was once again selected through LOOIC and deviance followed by a comparison of each respective model's deviance. Estimates from other models and deviance values are summarized in Table 5 and Table 6.

31

3.3.3   Madewell *et al*. Data

Employing the same techniques as previously outlined, I estimated the mean interval between exposure and rash onset for a study by Madewell *et al*. [25], but the exposure-to-symptom onset period was not estimated in the present study as the authors already provide their own estimates. In Madewell *et al.*, 12 state and local health departments provided self-reported data on symptom and rash onset dates for primary and secondary cases, with a focus on the specificity of rash onset for mpox. The data included cases where there was a high degree of certainty that the secondary case-patient was infected by the primary case-patient. Out of 120 case pairs from 13 jurisdictions, 57 pairs met the inclusion criteria required by the authors, with dates of symptom onset ranging from May 11 to August 13, 2022. Among the 57 pairs, 40 pairs had available rash onset dates for both primary and secondary case-patients.

Applying MCMC simulations to this study's data, the log-normal distribution model proved to be the best-fit model. Distribution model estimates and deviance values used for best-fit model selection are summarized in Table 5 and Table 6.

3.3.4   Viedma-Martinez *et al*. Data

Data from the tattoo parlor in Spain demonstrated that the mean exposure-to-rash onset period is not significantly best fitted to any of the distribution models. The deviance values for the Weibull, log-normal, and gamma distribution models are summarized in Table 6.

3.4   Meta-analysis

Parameter estimates pertaining to each study were selected from the best-fit model LOOIC selection method. When the data did not fit any model significantly better than the

<div align="center">32</div>

others, the log-normal model was selected, as it was the most common best-fit model for these epidemiological parameters.

First, the frequentist meta-analysis using the DL method was performed, and corresponding point estimates and values with 95% credible intervals are reported in forest plot form (Fig. 5A). With this frequentist approach, the I^2 statistic was also calculated to measure the total heterogeneity that is not accounted for by sampling error, and resulted in $I^2 = 57.1\%$. Additionally, the Q statistic was computed to assess the statistical significance of heterogeneity, yielding a value of 9.3 with 4 degrees of freedom and a p-value of 0.053. Although the I^2 statistic suggests large heterogeneity between data sets, the Q value did not show a highly significant level of heterogeneity.

Next, to begin performing a Bayesian meta-analysis, weakly informative priors were assigned for μ and τ in (3). Then, each dataset's exposure-to-symptom onset period was assigned a different weight, as their weight may be influenced by their collection and statistical methods or their sample sizes. In this study, the standard error derived from the 95% CrI was used to assign weights, which is why the 95% CrI was part of the inclusion criteria for datasets in this meta-analysis.
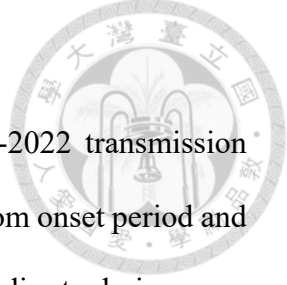
Afterwards, the estimated deviations of each dataset's "true" mean exposure-to-symptom onset period from the partially pooled model were estimated and a forest plot containing each dataset's IP distribution, mean, and 95% CrI was created. This forest plot also includes the partially pooled overarching distribution of IPs with its mean and lower and upper bounds of its 95% CrI are shown, as well as the distribution of the pre-2022 data set's posterior mean exposure-to-symptom onset period draws, for comparison purposes (Fig. 6A). These results revealed that the true mean exposure-to-symptom onset period estimations done on the data from Tarin-Vicente *et al.* [24] are least deviant from the partially pooled

33

exposure-to-symptom onset period distribution. The 95th, 97.5th, and 99th percentiles for posterior exposure-to-symptom onset period draws from the 2022-2023 studies were 15.5, 16.3, and 17.3 days, respectively.

Similar frequentist and Bayesian meta-analysis methods were applied to the mean exposure-to-rash onset period and resulted in a between-study heterogeneity of $I^2 = 48.3\%$. The three data sets with available rash onset dates were used for these meta-analyses. The pooled and partially pooled mean estimates for this parameter were calculated, and visualized on forest plots (Fig. 5B and Fig. 6B). For the Bayesian approach, the distribution of the posterior draws of the pre-2022 mean exposure-to-rash onset periods were also visualized. These results revealed that Tarin-Vicente *et al*. [24]'s data was closest to the partially pooled mean period length. The 95th, 97.5th, and 99th percentiles for the posterior exposure-to-rash onset period draws were 15.7, 16.9, and 20.4 days, respectively.
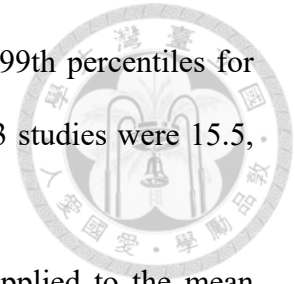
4 Discussion

The present study aimed to conduct a systematic review of pre-2022 transmission dynamics of mpox to derive an estimate for the mean exposure-to-symptom onset period and its standard deviation. Then, this study gathered data from a few other studies to derive more estimates of the mean exposure-to-symptom onset period and standard deviation from diverse populations of infected cases and the best-fit model, if there was one, for each dataset was selected after meticulous model assessment statistical methods. The estimates calculated through powerful statistical methods in this study were then compared through a frequentist and a hierarchical Bayesian meta-analysis with estimates calculated elsewhere. Ultimately, a pooled point estimate of the mean exposure-to-symptom onset period and partially pooled distribution of the mean exposure-to-symptom onset period was constructed and its mean and 95% credible intervals were derived. Furthermore, the mean length of the period between mpox exposure and onset of either a rash or other symptoms was also estimated where rash onset data were available as a secondary analysis of this study. A rash is much more indicative of mpox infection for many individuals, so this secondary analysis may have less uncertainty regarding the appropriate date of symptom onset for reported cases. Results revealed that the log-normal distribution most often best represents the distribution of these epidemiological parameters, and the mean exposure-to-symptom onset period of mpox infections for the 2022-2023 outbreaks is 7.8 days, and 8.5 days before 2022.
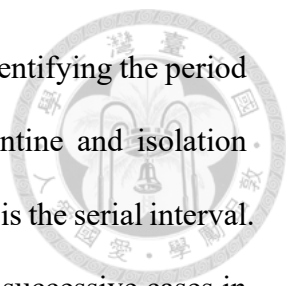
Initially, the mode of transmission of mpox was hypothesized to possibly influence the incubation period. For example, it was thought that complex modes of transmission, such as an mpox-infected needle penetrating the skin, may lead to a quicker presentation of symptoms. However, the analysis of the Viedma-Martinez *et al*. [22] dataset reveals that the

estimated mean exposure-to-symptom onset period is not far from the pooled mean exposure-to-symptom onset period, and it is actually slightly longer. This finding does not support the possibility that complex modes of transmission of mpox may lead to a significant difference in the time it takes for the presentation of symptoms.
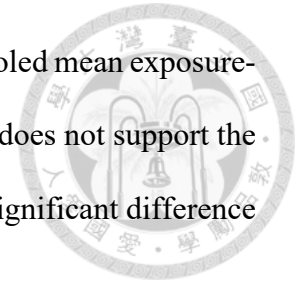
Noteworthy, Madewell *et al*., reported an exceptionally shorter exposure-to-symptom onset period. The cases for this study were all from the United States, and most of them reported exposure during international travel [25]. Only select cases were chosen for this data set: the ones with exact known exposure and onset dates, so their total number of reported cases was relatively small. Such strict selection may lead to bias which may have resulted in the observed short mean exposure-to-symptom onset period.

Compared to other datasets, the pre-2022 one did not have a mean exposure-to-symptom onset period particularly different from the pooled estimated value, but it was slightly longer. Many of the reported cases from before 2022 occurred by complex transmission—usually from a scratch or bite form an infected animal, which involved penetration of the skin tissue. This finding further suggests that, despite the difference in transmission mode, symptoms were not significantly quicker nor slower to appear among infected individuals, as the mean exposure-to-symptom onset period for the pre-2022 data is still within the 95% credible intervals of the partially pooled 2022-2023 cases. Nonetheless, there may be reporting biases associated with case interviews for any individuals in any of these datasets regarding exact dates of exposure and symptom onset, and a potential confusion between the onset of symptoms and rash onset, which could contribute to any observed differences in the estimated incubation periods. Further investigation is needed to assess the validity of these potential explanations.

Understanding the incubation period of a disease is important for identifying the period of highest risk of transmission and for determining appropriate quarantine and isolation measures. Another important epidemiological parameter to inform policy is the serial interval. As previously mentioned, the serial interval is the time interval between successive cases in a chain of transmission, while the incubation period is the time interval between exposure to an infectious individual and the onset of symptoms. If the serial interval is longer than the incubation period, it suggests that infected individuals are not transmitting mpox as quickly as they are becoming symptomatic. This could be due to a number of factors, including the infectiousness of the disease, the modes of transmission, and the behavior of the infected individuals. Mean serial intervals of mpox have been reported as generally longer than the estimated mean incubation periods [23], [25], [53], [54], which suggests that transmission of mpox likely occurs mostly after symptom onset. However, there have been cases where transmission was reported to have occurred before the infector's onset of symptoms [25], [53].

The estimated exposure-to-rash onset period distribution from the meta-analysis provided 90th, 95th, and 98th upper bound percentiles of 15.7, 16.9, and 20.4 days, respectively. Although the disease has a high transmissibility through various modes such as close contact, sharing of objects, food, drinks, and physical contact, given that most transmission cases occur after the presentation of rashes and a rash is a very apparent symptom, it seems reasonable to recommend that close contacts of confirmed cases do not need to undergo quarantine. For confirmed cases, a 21-day quarantine period should be initiated starting from the day after contact with the confirmed or suspected infector. This duration will cover the range after which most individuals develop discernible symptoms. Close contacts, on the other hand, may self-monitor their health for three weeks and be

increasingly cautious about any potential symptoms that may arise if they have had close contact with a confirmed case.

This study had certain limitations that need to be acknowledged. One of the major limitations was the unavailability of important data, such as the exact day of symptom onset or exposure from some of the extracted case data. To overcome this, Bayesian statistical methods, including MCMC sampling, were used. Despite the application of these methods, the estimated incubation periods may have still been affected by reporting bias, leading to inaccurate estimates. Bayesian methods adjust for this limitation by incorporating prior knowledge or beliefs about the data in the statistical model, which allows for the incorporation of external information and the adjustment of estimates based on the available data. However, the degree to which these limitations have impacted the results of the study is difficult to quantify, and future research with more accurate data may provide more precise estimates of the incubation period for mpox. Overall, the use of Bayesian statistics provides more accurate and precise estimates of the mean incubation period as opposed to other methods of estimation, which can have significant implications for controlling the spread of mpox. Performing a Bayesian meta-analysis provided more insight into a likely more accurate mean incubation period. However, the amount of heterogeneity and uncertainty within and between each dataset may have influenced the final result. A large benefit of the methods employed is that as new data become available, priors and other variables used in the present meta-analysis may be updated to revise the estimated incubation period.

The mode of transmission of mpox did not appear to affect the duration of the incubation period, as evidenced by this study's analyses. The estimated mean exposure-to-symptom onset period of 7.8 days can provide valuable insights for public health officials in determining the appropriate duration for quarantine measures. To enhance the precision of
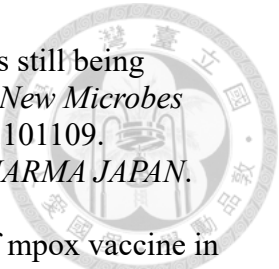
38

these estimates, future studies may focus on reducing uncertainties by implementing strategies to mitigate reporting biases, such as employing data collection methods that incorporate viral load modeling. Such efforts would contribute to a more comprehensive understanding of mpox and its associated epidemiological factors.
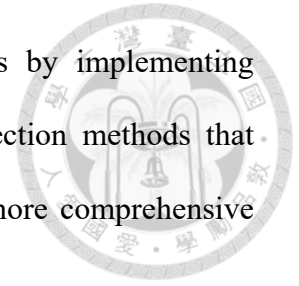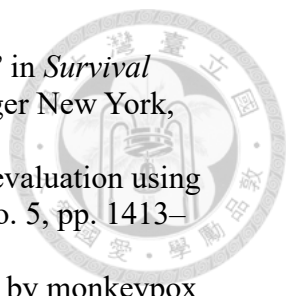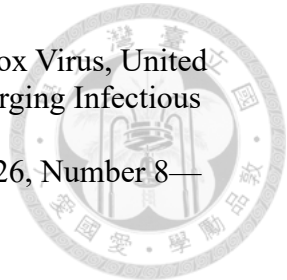
References

[1] "Update: Multistate Outbreak of Monkeypox --- Illinois, Indiana, Kansas, Missouri, Ohio, and Wisconsin, 2003." Accessed: Apr. 27, 2023. [Online]. Available: https://www.cdc.gov/mmwr/preview/mmwrhtml/mm5227a5.htm

[2] I. D. Ladnyj, P. Ziegler, and E. Kima, "A human infection caused by monkeypox virus in Basankusu Territory, Democratic Republic of the Congo," *Bull. World Health Organ.*, vol. 46, no. 5, pp. 593–597, 1972.

[3] "Mpox in the U.S.," *Centers for Disease Control and Prevention*, Jan. 06, 2023. https://www.cdc.gov/poxvirus/mpox/index.html (accessed Apr. 27, 2023).

[4] Z. Ježek and F. Fenner, *Human monkeypox*. in Monographs in virology, no. vol. 17. Basel ; New York: Karger, 1988.

[5] A. Yinka-Ogunleye *et al.*, "Reemergence of Human Monkeypox in Nigeria, 2017," *Emerg. Infect. Dis.*, vol. 24, no. 6, pp. 1149–1151, Jun. 2018, doi: 10.3201/eid2406.180017.

[6] P. E. M. FINE, Z. JEZEK, B. GRAB, and H. DIXON, "The Transmission Potential of Monkeypox Virus in Human Populations," *Int. J. Epidemiol.*, vol. 17, no. 3, pp. 643–650, Sep. 1988, doi: 10.1093/ije/17.3.643.

[7] "WHO Director-General declares the ongoing monkeypox outbreak a Public Health Emergency of International Concern." https://www.who.int/europe/news/item/23-07-2022-who-director-general-declares-the-ongoing-monkeypox-outbreak-a-public-health-event-of-international-concern (accessed May 27, 2023).

[8] "WHO recommends new name for monkeypox disease." https://www.who.int/news/item/28-11-2022-who-recommends-new-name-for-monkeypox-disease (accessed Apr. 27, 2023).

[9] J. G. Breman, "Monkeypox: an Emerging Infection for Humans?," in *Emerging Infections 4*, John Wiley & Sons, Ltd, 2000, pp. 45–67. doi: 10.1128/9781555816971.ch5.

[10] M. S. Maldonado *et al.*, "Epidemiologic characteristics and clinical features of patients with monkeypox virus infection from a hospital in Peru between July and September 2022," *Int. J. Infect. Dis.*, vol. 129, pp. 175–180, Apr. 2023, doi: 10.1016/j.ijid.2023.01.045.

[11] "2022-23 Mpox (Monkeypox) Outbreak: Global Trends." https://worldhealthorg.shinyapps.io/mpx_global/ (accessed Apr. 27, 2023).

[12] M. G. Reynolds *et al.*, "Clinical Manifestations of Human Monkeypox Influenced by Route of Infection," *J. Infect. Dis.*, vol. 194, no. 6, pp. 773–780, Sep. 2006, doi: 10.1086/505880.

[13] A. P. Riser *et al.*, "Epidemiologic and Clinical Features of Mpox-Associated Deaths — United States, May 10, 2022–March 7, 2023," *MMWR Morb. Mortal. Wkly. Rep.*, vol. 72, no. 15, pp. 404–410, Apr. 2023, doi: 10.15585/mmwr.mm7215a5.

[14] "Joint ECDC-WHO Regional Office for Europe Mpox Surveillance Bulletin." https://monkeypoxreport.ecdc.europa.eu/ (accessed Apr. 27, 2023).

[15] "Israel confirms first communal spread of monkeypox | The Times of Israel." https://www.timesofisrael.com/israel-confirms-first-communal-spread-of-monkeypox/ (accessed Apr. 27, 2023).

[16]   Md. S. Islam, A. M. M. T. Rahman, and Md. T. Rahman, "Mpox is still being neglected in South-East Asia region: Possible challenges to control," *New Microbes New Infect.*, vol. 52, p. 101109, Mar. 2023, doi: 10.1016/j.nmni.2023.101109.

[17]   "Mpox Cases Top 100 in Japan, 10 New Patients Confirmed," *PHARMA JAPAN*. https://pj.jiho.jp/article/248661 (accessed Apr. 27, 2023).

[18]   Y. Wolff Sagy *et al.*, "Real-world effectiveness of a single dose of mpox vaccine in males," *Nat. Med.*, vol. 29, no. 3, pp. 748–752, Mar. 2023, doi: 10.1038/s41591-023-02229-3.

[19]   "Monkeypox outbreak: India to screen arrival for virus signs, isolate sick patients; details here | India News | Zee News." https://zeenews.india.com/india/monkeypox-outbreak-india-to-screen-arrival-for-virus-signs-isolate-sick-patients-details-here-2465745.html (accessed Apr. 27, 2023).

[20]   "No monkeypox cases detected in Saudi Arabia, health ministry says." https://www.arabnews.com/node/2087001/saudi-arabia (accessed Apr. 27, 2023).

[21]   M. J. Page *et al.*, "The PRISMA 2020 statement: an updated guideline for reporting systematic reviews," *BMJ*, p. n71, Mar. 2021, doi: 10.1136/bmj.n71.

[22]   M. Viedma-Martinez *et al.*, "MPXV Transmission at a Tattoo Parlor," *N. Engl. J. Med.*, vol. 388, no. 1, pp. 92–94, Jan. 2023, doi: 10.1056/NEJMc2210823.

[23]   F. Miura *et al.*, "Estimated incubation period for monkeypox cases confirmed in the Netherlands, May 2022," *Eurosurveillance*, vol. 27, no. 24, Jun. 2022, doi: 10.2807/1560-7917.ES.2022.27.24.2200448.

[24]   E. J. Tarín-Vicente *et al.*, "Clinical presentation and virological assessment of confirmed human monkeypox virus cases in Spain: a prospective observational cohort study," *The Lancet*, vol. 400, no. 10353, pp. 661–669, Aug. 2022, doi: 10.1016/S0140-6736(22)01436-2.

[25]   Z. J. Madewell *et al.*, "Serial Interval and Incubation Period Estimates of Monkeypox Virus Infection in 12 Jurisdictions, United States, May–August 2022 - Volume 29, Number 4—April 2023 - Emerging Infectious Diseases journal - CDC", doi: 10.3201/eid2904.221622.

[26]   M. Harrer, *Doing meta-analysis with R: a hands-on guide*, First edition. Boca Raton: CRC Press, 2022.

[27]   R. DerSimonian and R. Kacker, "Random-effects model for meta-analysis of clinical trials: an update," *Contemp. Clin. Trials*, vol. 28, no. 2, pp. 105–114, Feb. 2007, doi: 10.1016/j.cct.2006.04.004.

[28]   Stan Development Team, "Stan Modeling Language Users Guide and Reference Manual." 2023. [Online]. Available: https://mc-stan.org

[29]   R Core Team, "R: A Language and Environment for Statistical Computing." R Foundation for Statistical Computing, Vienna, Austria, 2023. [Online]. Available: https://ww.R-project.org/

[30]   M. E. Halloran, M. Haber, I. M. Longini, and C. J. Struchiner, "Direct and Indirect Effects in Vaccine Efficacy and Effectiveness," *Am. J. Epidemiol.*, vol. 133, no. 4, pp. 323–331, Feb. 1991, doi: 10.1093/oxfordjournals.aje.a115884.

[31]   J. Peto *et al.*, "Universal weekly testing as the UK COVID-19 lockdown exit strategy," *The Lancet*, vol. 395, no. 10234, pp. 1420–1421, May 2020, doi: 10.1016/S0140-6736(20)30936-3.

[32]   J. P. Klein and M. L. Moeschberger, "Censoring and Truncation," in *Survival Analysis*, in Statistics for Biology and Health. New York, NY: Springer New York, 2003, pp. 63–90. doi: 10.1007/0-387-21645-6_3.

[33]   A. Vehtari, A. Gelman, and J. Gabry, "Practical Bayesian model evaluation using leave-one-out cross-validation and WAIC," *Stat. Comput.*, vol. 27, no. 5, pp. 1413–1432, Sep. 2017, doi: 10.1007/s11222-016-9696-4.

[34]   I. D. Ladnyj, P. Ziegler, and E. Kima, "A human infection caused by monkeypox virus in Basankusu Territory, Democratic Republic of the Congo," *Bull. World Health Organ.*, vol. 46, no. 5, pp. 593–597, 1972.

[35]   J. C. Kile *et al.*, "Article," *Arch. Pediatr. Adolesc. Med.*, vol. 159, no. 11, pp. 1022–1025, Nov. 2005, doi: 10.1001/archpedi.159.11.1022.

[36]   N. Erez *et al.*, "Diagnosis of Imported Monkeypox, Israel, 2018 - Volume 25, Number 5—May 2019 - Emerging Infectious Diseases journal - CDC", doi: 10.3201/eid2505.190076.

[37]   I. K. Damon, C. E. Roth, and V. Chowdhary, "Discovery of Monkeypox in Sudan," *N. Engl. J. Med.*, vol. 355, no. 9, pp. 962–963, Aug. 2006, doi: 10.1056/NEJMc060792.

[38]   R. H. Doshi *et al.*, "Epidemiologic and Ecologic Investigations of Monkeypox, Likouala Department, Republic of the Congo, 2017 - Volume 25, Number 2—February 2019 - Emerging Infectious Diseases journal - CDC", doi: 10.3201/eid2502.181222.

[39]   A. T. Fleischauer *et al.*, "Evaluation of Human-to-Human Transmission of Monkeypox from Infected Patients to Health Care Workers," *Clin. Infect. Dis.*, vol. 40, no. 5, pp. 689–694, Mar. 2005, doi: 10.1086/427805.

[40]   "Exportation of Monkeypox Virus From the African Continent | The Journal of Infectious Diseases | Oxford Academic." https://academic.oup.com/jid/article/225/8/1367/5901023?login=true (accessed Apr. 30, 2023).

[41]   L. D. Nolen *et al.*, "Extended Human-to-Human Transmission during a Monkeypox Outbreak in the Democratic Republic of the Congo - Volume 22, Number 6—June 2016 - Emerging Infectious Diseases journal - CDC", doi: 10.3201/eid2206.150579.

[42]   G. Hobson *et al.*, "Family cluster of three cases of monkeypox imported from Nigeria to the United Kingdom, May 2021," *Eurosurveillance*, vol. 26, no. 32, p. 2100745, Aug. 2021, doi: 10.2807/1560-7917.ES.2021.26.32.2100745.

[43]   Z. Jezek, I. Arita, M. Mutombo, C. Dunn, J. H. Nakano, and M. Szczeniowski, "Four generations of probable person-to-person transmission of human monkeypox," *Am. J. Epidemiol.*, vol. 123, no. 6, pp. 1004–1012, Jun. 1986, doi: 10.1093/oxfordjournals.aje.a114328.

[44]   S. O. Foster *et al.*, "Human monkeypox," *Bull. World Health Organ.*, vol. 46, no. 5, pp. 569–576, 1972.

[45]   P. Formenty *et al.*, "Human Monkeypox Outbreak Caused by Novel Virus Belonging to Congo Basin Clade, Sudan, 2005 - Volume 16, Number 10—October 2010 - Emerging Infectious Diseases journal - CDC", doi: 10.3201/eid1610.100713.

[46]   M. Mutombo, Z. Jezek, I. Arita, and Z. Jezek, "HUMAN MONKEYPOX TRANSMITTED BY A CHIMPANZEE IN A TROPICAL RAIN-FOREST AREA OF ZAIRE," *The Lancet*, vol. 321, no. 8327, pp. 735–737, Apr. 1983, doi: 10.1016/S0140-6736(83)92027-5.

[47] A. Vaughan *et al.*, "Human-to-Human Transmission of Monkeypox Virus, United Kingdom, October 2018 - Volume 26, Number 4—April 2020 - Emerging Infectious Diseases journal - CDC", doi: 10.3201/eid2604.191164.

[48] S. E. F. Yong *et al.*, "Imported Monkeypox, Singapore - Volume 26, Number 8—August 2020 - Emerging Infectious Diseases journal - CDC", doi: 10.3201/eid2608.191387.

[49] "Monkeypox - the United States of America." https://www.who.int/emergencies/disease-outbreak-news/item/monkeypox---the-united-states-of-america (accessed Apr. 30, 2023).

[50] "Monkeypox - United Kingdom of Great Britain and Northern Ireland ex Nigeria." https://www.who.int/emergencies/disease-outbreak-news/item/monkeypox---united-kingdom-of-great-britain-and-northern-ireland-ex-nigeria (accessed Apr. 30, 2023).

[51] G. Froeschl and P. K. Kayembe, "Pox-like lesions and haemorrhagic fever in two concurrent cases in the Central African Republic: case investigation and management in difficult circumstances," *Pan Afr. Med. J.*, vol. 22, no. 23, Art. no. 23, Oct. 2015, doi: 10.11604/pamj.2015.22.23.6620.

[52] K. D. Reed *et al.*, "The Detection of Monkeypox in Humans in the Western Hemisphere," *N. Engl. J. Med.*, vol. 350, no. 4, pp. 342–350, Jan. 2004, doi: 10.1056/NEJMoa032299.

[53] T. Ward, R. Christie, R. S. Paton, F. Cumming, and C. E. Overton, "Transmission dynamics of monkeypox in the United Kingdom: contact tracing study," *BMJ*, p. e073153, Nov. 2022, doi: 10.1136/bmj-2022-073153.

[54] Z. Guo, S. Zhao, S. Sun, D. He, K. C. Chong, and E. K. Yeoh, "Estimation of the serial interval of monkeypox during the early outbreak in 2022," *J. Med. Virol.*, vol. 95, no. 1, p. e28248, 2023, doi: 10.1002/jmv.28248.

Appendix

Stan code for the Weibull, log-normal, and gamma distribution models fit to
   (1) Pre-2022 data
            a.   Exposure-to-symptom onset period (gamma):

```
data {
  int<lower = 1> N_obs; // number of complete rows
  vector[N_obs] EL_obs, ER_obs, OL_obs, OR_obs; // left and right boundaries for
observed exposure and onset dates
  int<lower = 1> N_cens; // number of rows with missing observations
  vector[N_cens] ER_cens, OL_cens, OR_cens; // exposure and onset dates with
missing observations
}

transformed data {
  int N = N_obs + N_cens; // total number of rows
  vector[N] ER = append_row(ER_obs, ER_cens) + 1, // right boundary of exposure
dates
           OL = append_row(OL_obs, OL_cens), // left boundary of onset dates
           OR = append_row(OR_obs, OR_cens) + 1; // right boundary of onset
dates
}

parameters {
  real<lower = 0> alpha, beta; // shape and rate parameters for the gamma
distribution

  // parameters to sample intervals between left and right boundaries of
exposure and onset dates, respectively
  vector<lower = 0, upper = 1>[N] e_raw, o_raw;

  vector<lower = 0>[N_cens] EL_cens_raw; // missing left boundary exposure dates
}

transformed parameters {
  real mean_ip = alpha / beta; // mean exposure-to-symptom onset period, gamma-
distributed
  real sd_ip = sqrt(alpha / (beta^2)); // standard deviation of the exposure-to-
symptom onset period
  vector[N_cens] EL_cens = -EL_cens_raw;
  vector[N] EL = append_row(EL_obs, EL_cens); // all left boundary exposure
dates
}

model {
  // gamma distribution model priors
  e_raw ~ uniform(0,1);
  o_raw ~ uniform(0,1);
  alpha ~ gamma(0.001, 0.001);
  beta ~ gamma(0.001, 0.001);

  // weakly informative prior distribution for the missing observations
  EL_cens_raw ~ exponential(0.01);
```

44

```
  vector[N] e = EL + (ER - EL) .* e_raw; // vector of exposure dates
  vector[N] o = OL + (OR - OL) .* o_raw; // vector of symptom onset dates
  target += gamma_lpdf(o - e | alpha, beta);
}

generated quantities {
  vector[N] e = EL + (ER - EL) .* e_raw;
  vector[N] o = OL + (OR - OL) .* o_raw;
  real log_lik;
  log_lik = gamma_lpdf(o - e | alpha, beta); // log-likelihood of observing the
posterior values
}
```

b. Exposure-to-rash onset period (Weibull):

```
data {
  int<lower = 1> N_obs; // number of complete rows
  vector[N_obs] EL_obs, ER_obs, OL_obs, OR_obs; // left and right boundaries for
observed exposure and rash onset dates
  int<lower = 1> N_cens; // number of rows with missing observations
  vector[N_cens] ER_cens, OL_cens, OR_cens; // exposure and rash onset dates
with missing observations
}

transformed data {
  int N = N_obs + N_cens; // total number of rows
  vector[N] ER = append_row(ER_obs, ER_cens) + 1, // right boundary of exposure
dates
           OL = append_row(OL_obs, OL_cens), // left boundary of rash onset
dates
           OR = append_row(OR_obs, OR_cens) + 1; // right boundary of rash
onset dates
}

parameters {
  real<lower = 0> lambda, k; // scale and shape parameters for the gamma
distribution

  // parameters to sample intervals between left and right boundaries of
exposure and rash onset dates, respectively
  vector<lower = 0, upper = 1>[N] e_raw, o_raw;

  vector<lower = 0>[N_cens] EL_cens_raw; // missing left boundary exposure dates
}

transformed parameters {
  real mean_rash = lambda * tgamma(1 + 1/k); // mean exposure-to-rash onset
length, Weibull-distributed
  vector[N_cens] EL_cens = -EL_cens_raw;
  vector[N] EL = append_row(EL_obs, EL_cens); // all left boundary exposure
dates
}

model {
  // set priors
  e_raw ~ uniform(0,1);
```

```
  o_raw ~ uniform(0,1);
  lambda ~ normal(0, 10);
  k ~ cauchy(0, 10);

  // weakly informative prior distribution for the missing observations
  EL_cens_raw ~ exponential(0.01);

  vector[N] e = EL + (ER - EL) .* e_raw; // vector of exposure dates
  vector[N] o = OL + (OR - OL) .* o_raw; // vector of symptom onset dates
  target += weibull_lpdf(o - e | k, lambda);
}

generated quantities {
  // standard deviation of exposure-to-rash onset length for the Weibull
distribution
  real sd_rash = sqrt(lambda^2 * (tgamma(1 + 2/k) - (tgamma(1 + 1/k)^2)));

  vector[N] e = EL + (ER - EL) .* e_raw;
  vector[N] o = OL + (OR - OL) .* o_raw;
  real log_lik;
  log_lik = weibull_lpdf(o - e | k, lambda); // log-likelihood of observing the
posterior values
}
```

(2) Viedma-Martinez *et al.* (2023) data

      a.   Exposure-to-symptom onset period (log-normal):

```
data {
  int<lower=1> N; // number of observations
  vector[N] EL; // exposure left boundaries
  vector[N] OL; // onset left boundaries
}

transformed data {
  vector[N] OR = OL + 1, ER = EL + 1; // symptom onset and exposure right
boundaries
}

parameters {
  // parameters to sample intervals between left and right boundaries of
exposure and onset dates, respectively
  vector<lower=0, upper=1>[N] e_raw, o_raw;

  real<lower=0> mu;        // location parameter
  real<lower=0> sigma;     // scale parameter
}

transformed parameters {
  real mean_ip = exp(mu + (sigma^2)/2); // mean exposure-to-symptom onset period
for the lognormal distribution
  real sd_ip = sqrt((exp(sigma^2) - 1) * exp(2 * mu + sigma^2)); // standard
deviation of the exposure-to-symptom onset period
}

model {
```

```
  // set priors
  e_raw ~ uniform(0,1);
  o_raw ~ uniform(0,1);
  mu ~ normal(5, 10);
  sigma ~ cauchy(0,5);

  vector[N] e = EL + (ER - EL) .* e_raw, o = OL + (OR - OL) .* o_raw;
  target += lognormal_lpdf(o - e | mu, sigma);
}

generated quantities {
  vector[N] e = EL + (ER - EL) .* e_raw;
  vector[N] o = OL + (OR - OL) .* o_raw;
  real log_lik;
  log_lik = lognormal_lpdf(o - e | mu, sigma); // log-likelihood for the log-
normal PDF
}
```

        b.   Exposure-to-rash onset period (gamma):

```
data {
  int<lower=1> N; // number of observations
  vector[N] EL; // exposure left boundaries
  vector[N] OL; // rash onset left boundaries
}

transformed data {
  vector[N] OR = OL + 1, ER = EL + 1; // rash onset and exposure right
boundaries, respectively
}

parameters {
  vector<lower=0, upper=1>[N] e_raw, o_raw;
  real<lower=0> alpha; // shape parameter
  real<lower=0> beta; // rate parameter
}

transformed parameters {
  real mean_rash = alpha / beta; // mean exposure-to-rash onset length, gamma-
distributed
  real sd_rash = sqrt(alpha / (beta^2)); // standard deviation of exposure-to-
rash onset length
}

model {
  // set priors
  e_raw ~ uniform(0,1);
  o_raw ~ uniform(0,1);
  alpha ~ gamma(0.001, 0.001);
  beta ~ gamma(0.001, 0.001);

  vector[N] e = EL + (ER - EL) .* e_raw, o = OL + (OR - OL) .* o_raw; // vectors
of exposure and rash onset dates
  target += gamma_lpdf(o - e | alpha, beta);
}
```

```
generated quantities {
  vector[N] e = EL + (ER - EL) .* e_raw;
  vector[N] o = OL + (OR - OL) .* o_raw;
  real log_lik;
  log_lik = gamma_lpdf(o - e | alpha, beta); // log-likelihood of observing the
posterior values
}
```

(3) Miura *et al.* (2022) data

        a. Exposure-to-symptom onset period (log-normal):

```
data {
  int<lower=1> N; // number of observations
  vector[N] EL; // exposure left boundaries
  vector[N] ER_raw; // exposure right boundaries
  vector[N] OL; // onset times
}

transformed data {
  vector[N] OR = OL + 1, ER; // onset right boundaries and new exposure right
boundaries

  for (i in 1:N) {
    if (EL[i] == ER_raw[i]) {
      ER[i] = ER_raw[i] + 1; // add one day to exposure right boundaries to
account for time variablity
    } else {
      ER[i] = ER_raw[i];
    }
  }
}

parameters {
  // parameters to sample intervals between left and right boundaries of
exposure and onset dates, respectively
  vector<lower=0, upper=1>[N] e_raw, o_raw;

  real<lower=0> mu; // location parameter
  real<lower=0> sigma; // scale parameter
}

transformed parameters {
  real mean_ip = exp(mu + (sigma^2)/2); // mean exposure-to-symptom onset period
for the lognormal distribution
  real sd_ip = sqrt((exp(sigma^2) - 1) * exp(2 * mu + sigma^2)); // standard
deviation of the exposure-to-symptom onset period
}

model {
  // set priors
  e_raw ~ uniform(0,1);
  o_raw ~ uniform(0,1);
  mu ~ normal(5, 10);
  sigma ~ cauchy(0,5);
```

<center>48</center>

```
    vector[N] e = EL + (ER - EL) .* e_raw, o = OL + (OR - OL) .* o_raw;
    target += lognormal_lpdf(o - e | mu, sigma);
}

generated quantities {
  vector[N] e = EL + (ER - EL) .* e_raw;
  vector[N] o = OL + (OR - OL) .* o_raw;
  real log_lik;
  log_lik = lognormal_lpdf(o - e | mu, sigma); // log-likelihood for the log-
normal PDF
```

    (4) Tarin-Vicente *et al*. (2023) data
        a. Exposure-to-symptom onset period; right truncation adjustment (gamma):

```
data {
  int<lower = 1> N; // number of observations
  vector[N] EL, OL; // exposure and symptom onset left boundaries, respectively
}

transformed data {
  vector[N] ER = EL + 1, OR = OL + 1; // exposure and symptom onset right
boundaries, respectively
  real trunc_day = max(OL); // truncation day set as the last date of data
collection (last day of recorded symptom onset)
}

parameters {
  real<lower = 0> alpha, beta; // shape and rate parameters for the gamma
distribution

  // parameters to sample intervals between left and right boundaries of
exposure and onset dates, respectively
  vector<lower = 0, upper = 1>[N] e_raw, o_raw;
}

transformed parameters {
  real mean_ip = alpha / beta; // mean exposure-to-symptom onset period, gamma-
distributed
  real sd_ip = sqrt(alpha / (beta^2)); // standard deviation of the exposure-to-
symptom onset period
}

model {
  // gamma distribution model priors
  e_raw ~ uniform(0,1);
  o_raw ~ uniform(0,1);
  alpha ~ gamma(0.001, 0.001);
  beta ~ gamma(0.001, 0.001);

  vector[N] e = EL + (ER - EL) .* e_raw; // vector of exposure dates
  vector[N] o = OL + (OR - OL) .* o_raw; // vector of symptom onset dates
  target += gamma_lpdf(o - e | alpha, beta) - gamma_lcdf(trunc_day + 1 - e |
alpha, beta);
}
```

```
generated quantities {
  vector[N] e = EL + (ER - EL) .* e_raw;
  vector[N] o = OL + (OR - OL) .* o_raw;
  real log_lik;
  log_lik = gamma_lpdf(o - e | alpha, beta) - gamma_lcdf(trunc_day + 1 - e |
alpha, beta); // log-likelihood of observing the posterior values
}
```

     b. Exposure-to-rash onset period; right truncation adjustment (Weibull):

```
data {
  int<lower = 1> N; // number of observations
  vector[N] EL, OL; // exposure and rash onset left boundaries, respectively
}

transformed data {
  vector[N] ER = EL + 1, OR = OL + 1; // exposure and rash onset right
boundaries, respectively
  real trunc_day = max(OL); // truncation day set as the last date of data
}

parameters {
  real<lower = 0> lambda, k; // scale and shape parameters for the gamma
distribution

  // parameters to sample intervals between left and right boundaries of
exposure and rash onset dates, respectively
  vector<lower = 0, upper = 1>[N] e_raw, o_raw;
}

transformed parameters {
  real mean_rash = lambda * tgamma(1 + 1/k); // mean exposure-to-rash onset
length, Weibull-distributed
}

model {
  // set priors
  e_raw ~ uniform(0,1);
  o_raw ~ uniform(0,1);
  lambda ~ normal(0, 10);
  k ~ cauchy(0, 10);

  vector[N] e = EL + (ER - EL) .* e_raw; // vector of exposure dates
  vector[N] o = OL + (OR - OL) .* o_raw; // vector of symptom onset dates
  target += weibull_lpdf(o - e | k, lambda) – weibull_lcdf(o – e | k, lambda);
}

generated quantities {
  // standard deviation of exposure-to-rash onset length for the Weibull
distribution
  real sd_rash = sqrt(lambda^2 * (tgamma(1 + 2/k) - (tgamma(1 + 1/k)^2)));

  vector[N] e = EL + (ER - EL) .* e_raw;
  vector[N] o = OL + (OR - OL) .* o_raw;
  real log_lik;
```

```
log_lik = weibull_lpdf(o - e | k, lambda) - weibull_lcdf(o - e | k, lambda);
// log-likelihood of observing the posterior values with right truncation
}
```

(5) Madewell *et al*. (2022) data

      a.   Exposure-to-rash onset period (log-normal):

```
data {
  int<lower = 1> N; // number of observations
  vector[N] EL, ER, OL, OR; // left and right exposure and rash onset dates,
respectively
}

parameters {
  // parameters to sample intervals between left and right boundaries of
exposure and onset dates, respectively
  vector<lower=0, upper=1>[N] e_raw, o_raw;

  real<lower=0> mu; // location parameter
  real<lower=0> sigma; // scale parameter
}

transformed parameters {
  real mean_rash = exp(mu + (sigma^2)/2); // mean exposure-to-rash length for
the lognormal distribution
  real sd_rash = sqrt((exp(sigma^2) - 1) * exp(2 * mu + sigma^2)); // standard
deviation of the exposure-to-rash length
}

model {
  // set priors
  e_raw ~ uniform(0,1);
  o_raw ~ uniform(0,1);
  mu ~ normal(5, 10);
  sigma ~ cauchy(0,5);

  vector[N] e = EL + (ER - EL) .* e_raw, o = OL + (OR - OL) .* o_raw;
  target += lognormal_lpdf(o - e | mu, sigma);
}

generated quantities {
  vector[N] e = EL + (ER - EL) .* e_raw;
  vector[N] o = OL + (OR - OL) .* o_raw;
  real log_lik;
  log_lik = lognormal_lpdf(o - e | mu, sigma); // log-likelihood for the log-
normal PDF
}
```
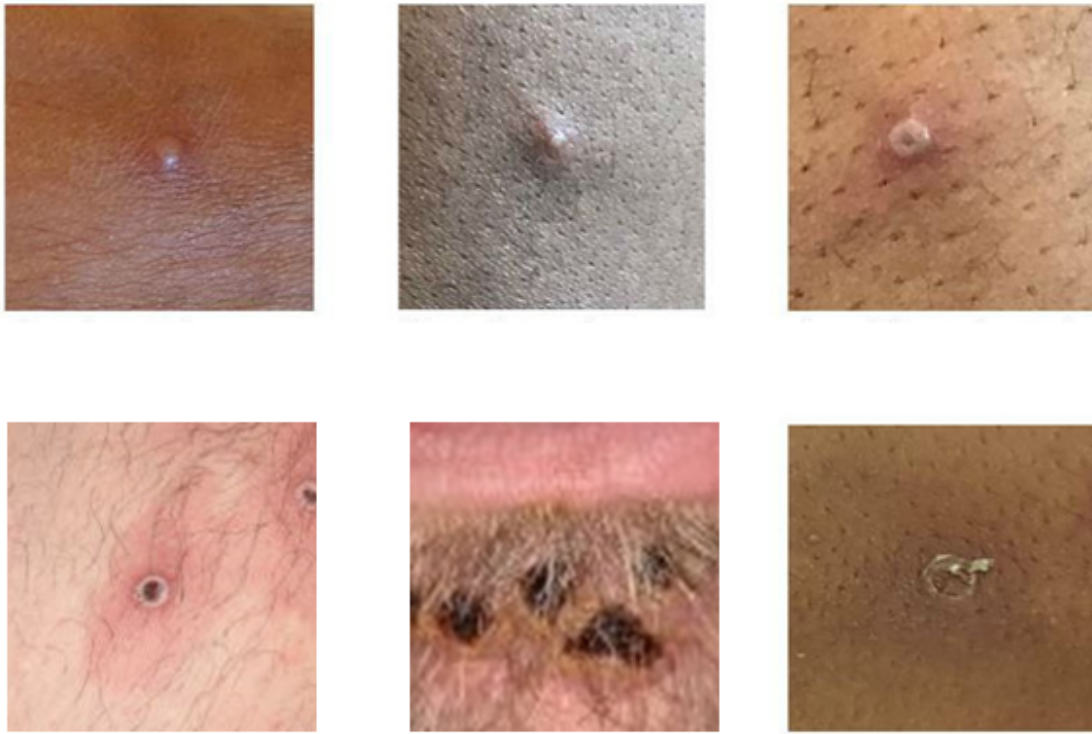
Tables & Figures

Fig. 1 Rash presentation of mpox. Adapted from [3].

331 records identified through database searching
1 record identified through other searches

332 records screened

240 records excluded by title and abstract
236 unrelated
4 inaccessible

92 full-text records assessed for eligibility

73 full-text articles excluded
55 without information on individual cases
18 without information on definitive exposure

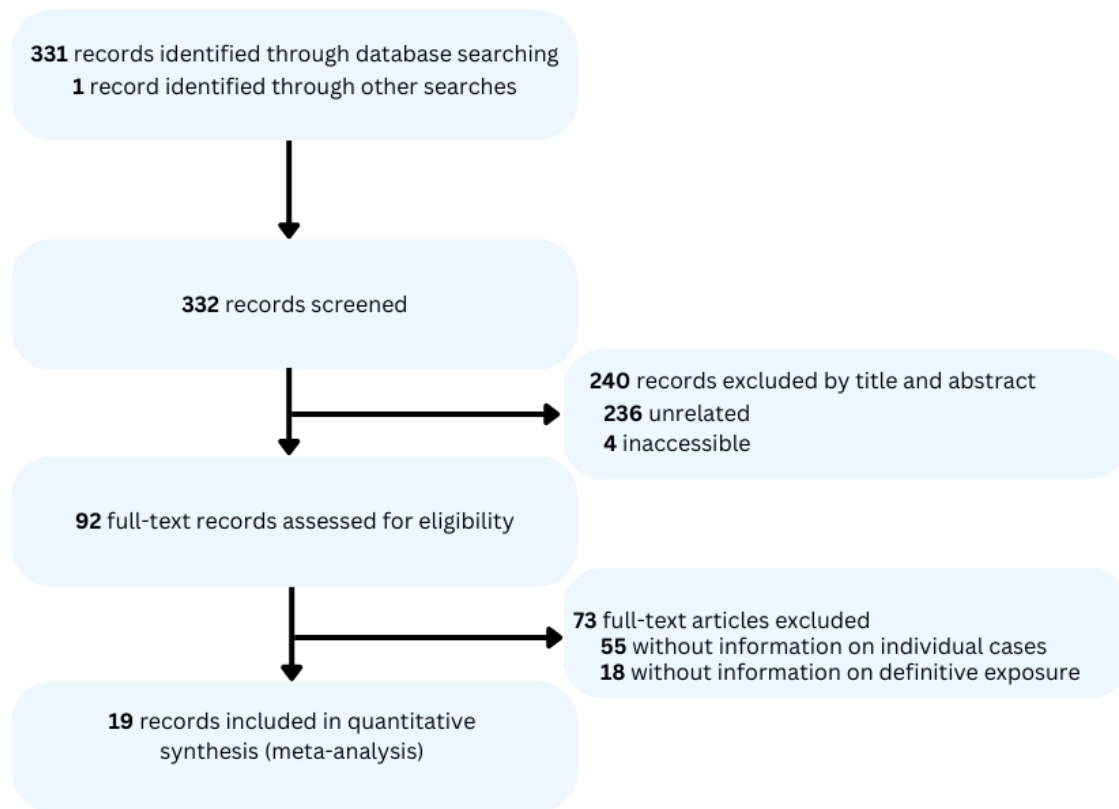19 records included in quantitative synthesis (meta-analysis)
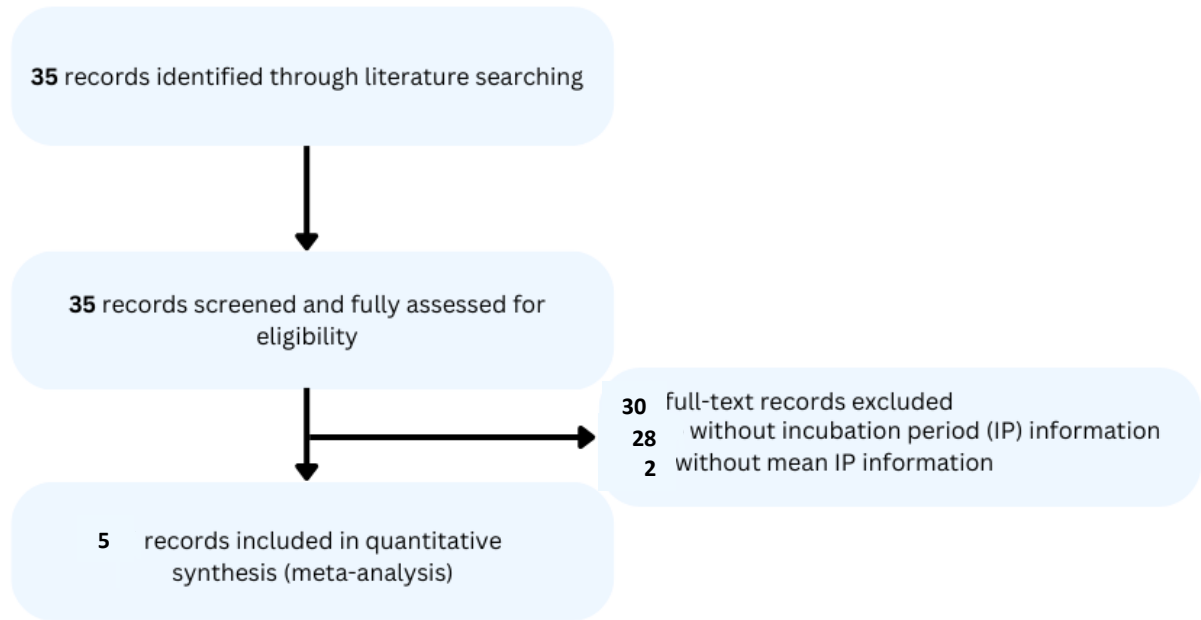
Fig. 2 Flow diagram for pre-2022 mpox transmission cases.

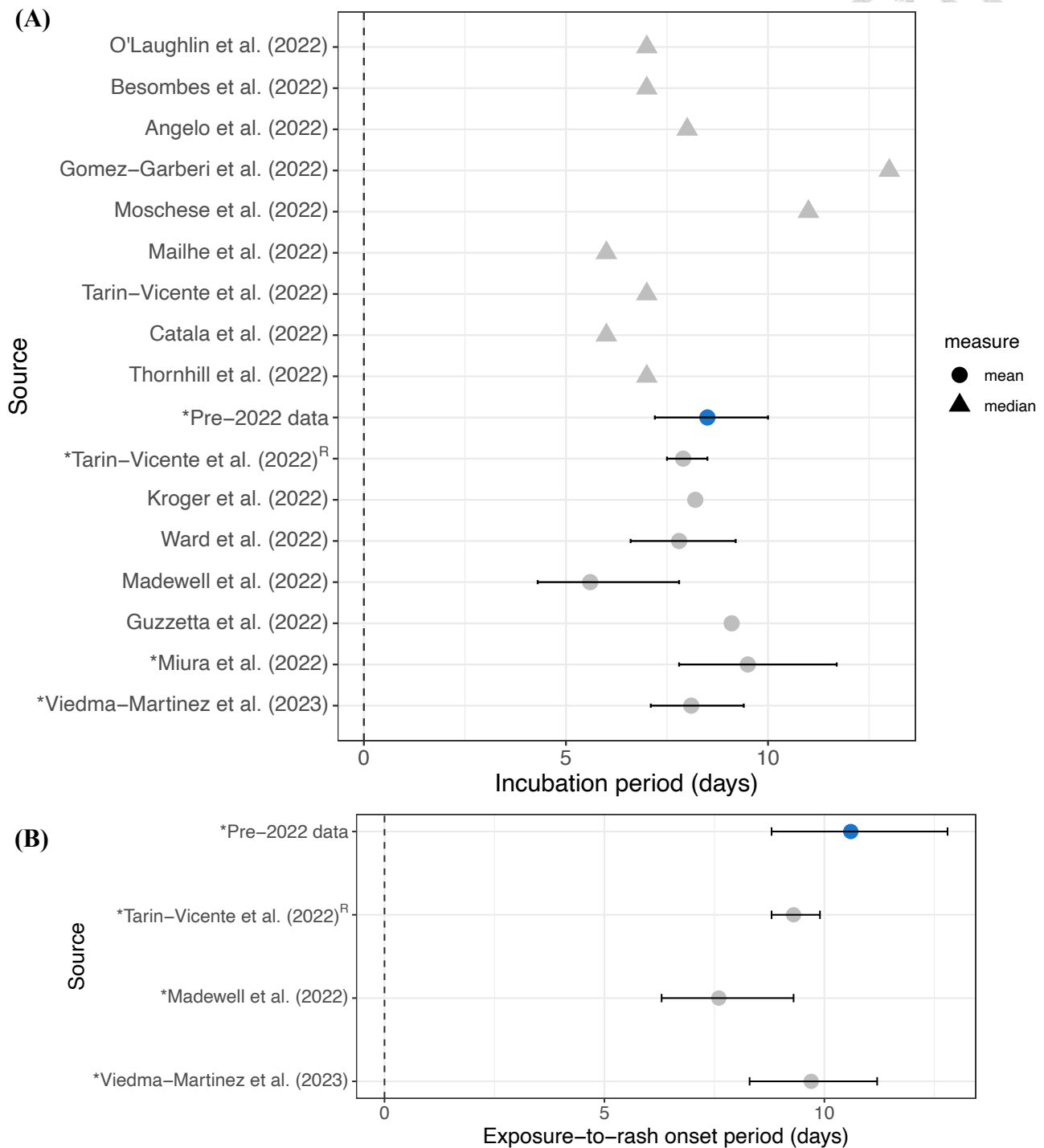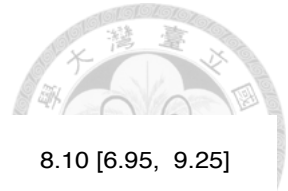Fig. 3 Flow diagram for current mpox epidemic incubation period estimates.

Fig. 4 **(A)** Forest plot of estimated mpox exposure-to-symptom onset periods with their 95% credible intervals. The estimated median IPs are represented as triangles, while the mean IPs are represented as circles with 95% credible interval bars. **(B)** Forest plot of estimated mpox exposure-to-rash onset periods with their 95% credible intervals. Kroger et al.'s study has not yet been peer-reviewed. The rows marked with * represent the estimates calculated in this study. The blue point is the estimate of the mean exposure-to-symptom onset period from cases before the 2022-2023 outbreaks. The superscript "R" represents that the data was adjusted for right truncation.

(A)

Ward et al. (2022)		8.10 [6.95, 9.25]
Viedma-Martinez et al. (2023)		9.50 [7.55, 11.45]
Miura et al. (2022)		5.60 [3.85, 7.35]
Madewell et al. (2022)		7.90 [7.40, 8.40]
Tarin-Vicente et al. (2022)		7.80 [6.50, 9.10]
Pooled Model		7.80 [6.98, 8.61]

Incubation period length (days)

(B)

Viedma-Martinez et al. (2023)		9.50 [8.25, 10.75]
Madewell et al. (2022)		7.60 [6.10, 9.10]
Tarin-Vicente et al. (2023)		9.00 [8.45, 9.55]
Pooled Model		8.84 [7.99, 9.68]

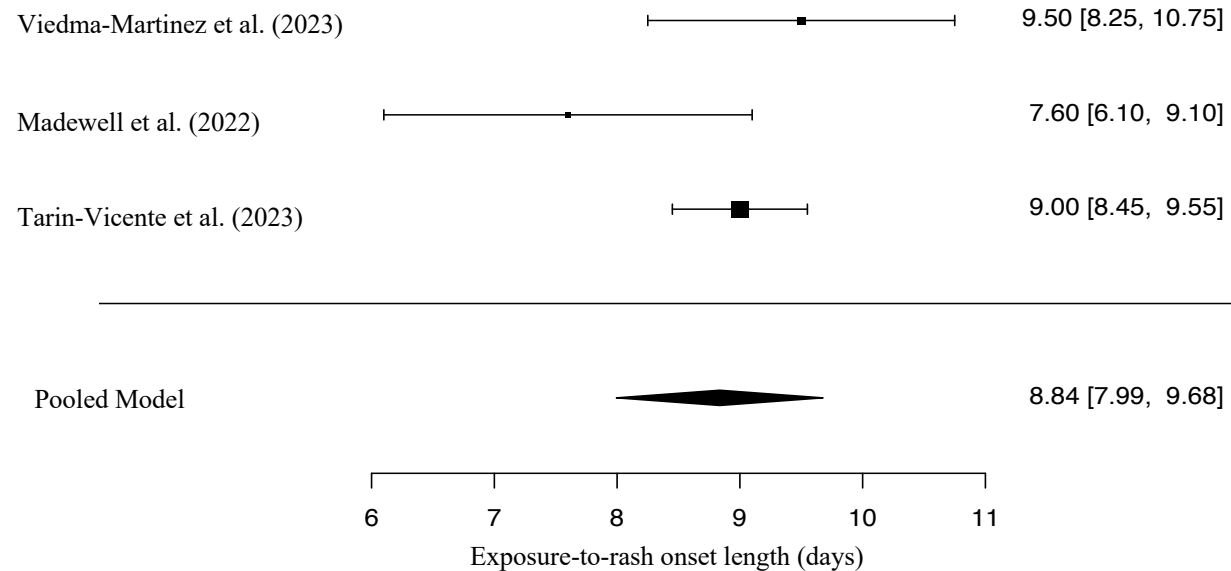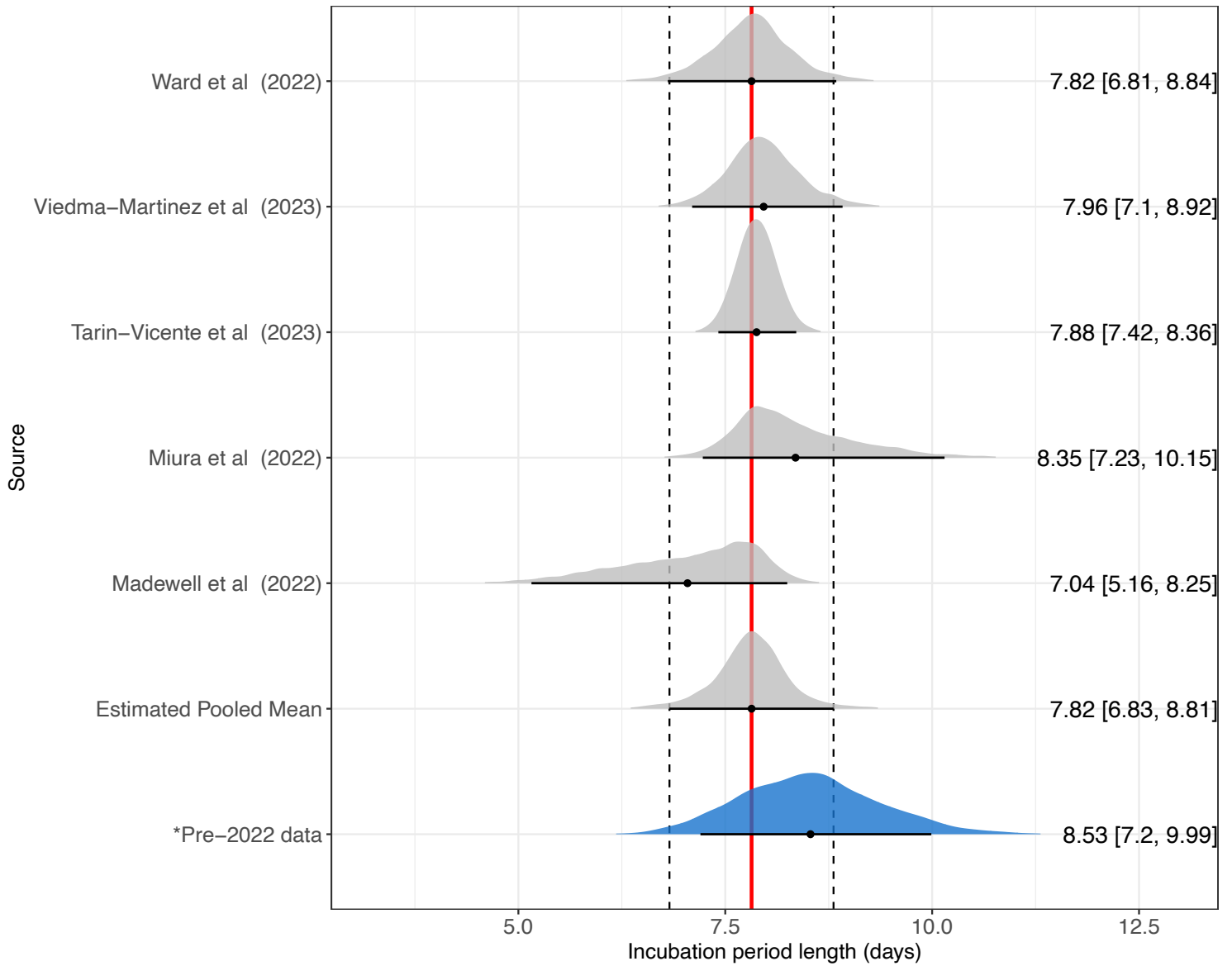Exposure-to-rash onset length (days)
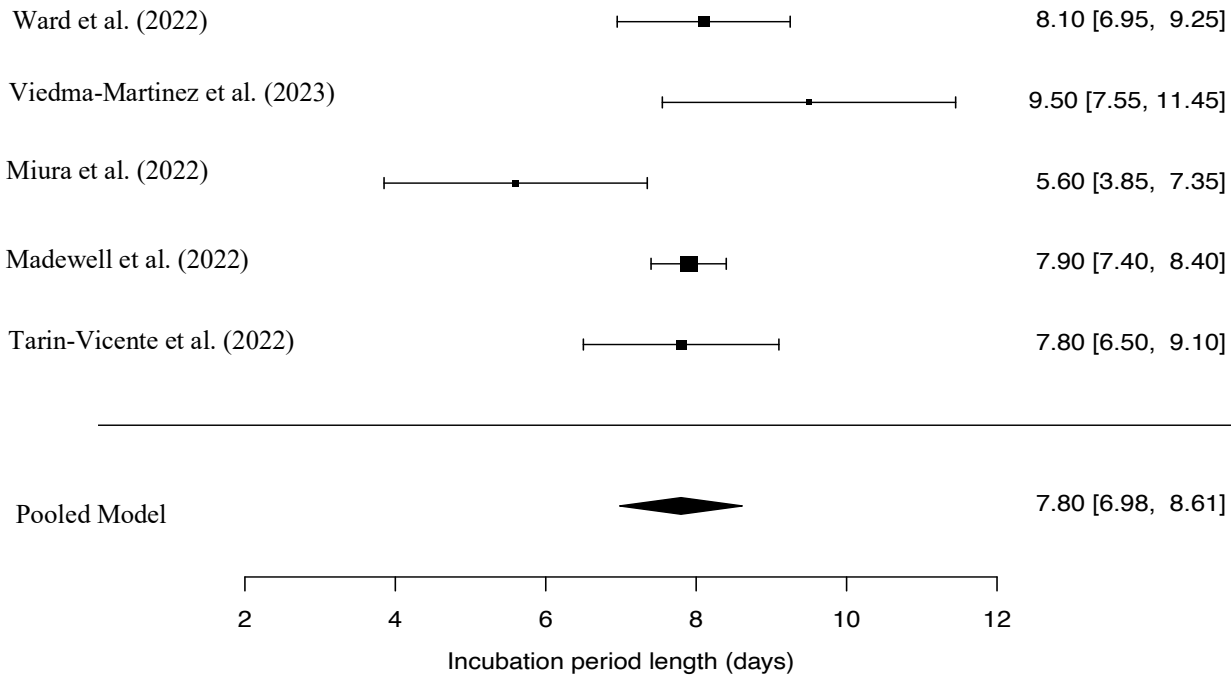
Fig. 5 Forest plot displaying the estimated **(A)** mean exposure-to-symptom onset period length (days) and **(B)** mean exposure-to-rash onset length for studies that met the inclusion criteria. The mean values are represented by the squares, and the horizontal lines indicate the 95% credible intervals around the mean estimates. The size of each square reflects the precision of the estimate, with larger squares indicating smaller standard errors. The diamond at the bottom represents the overall pooled mean estimate, and its width represents the corresponding confidence interval. The random-effects model (method of DerSimonian and Laird) was used to combine the study-specific estimates.

(A)

(B)
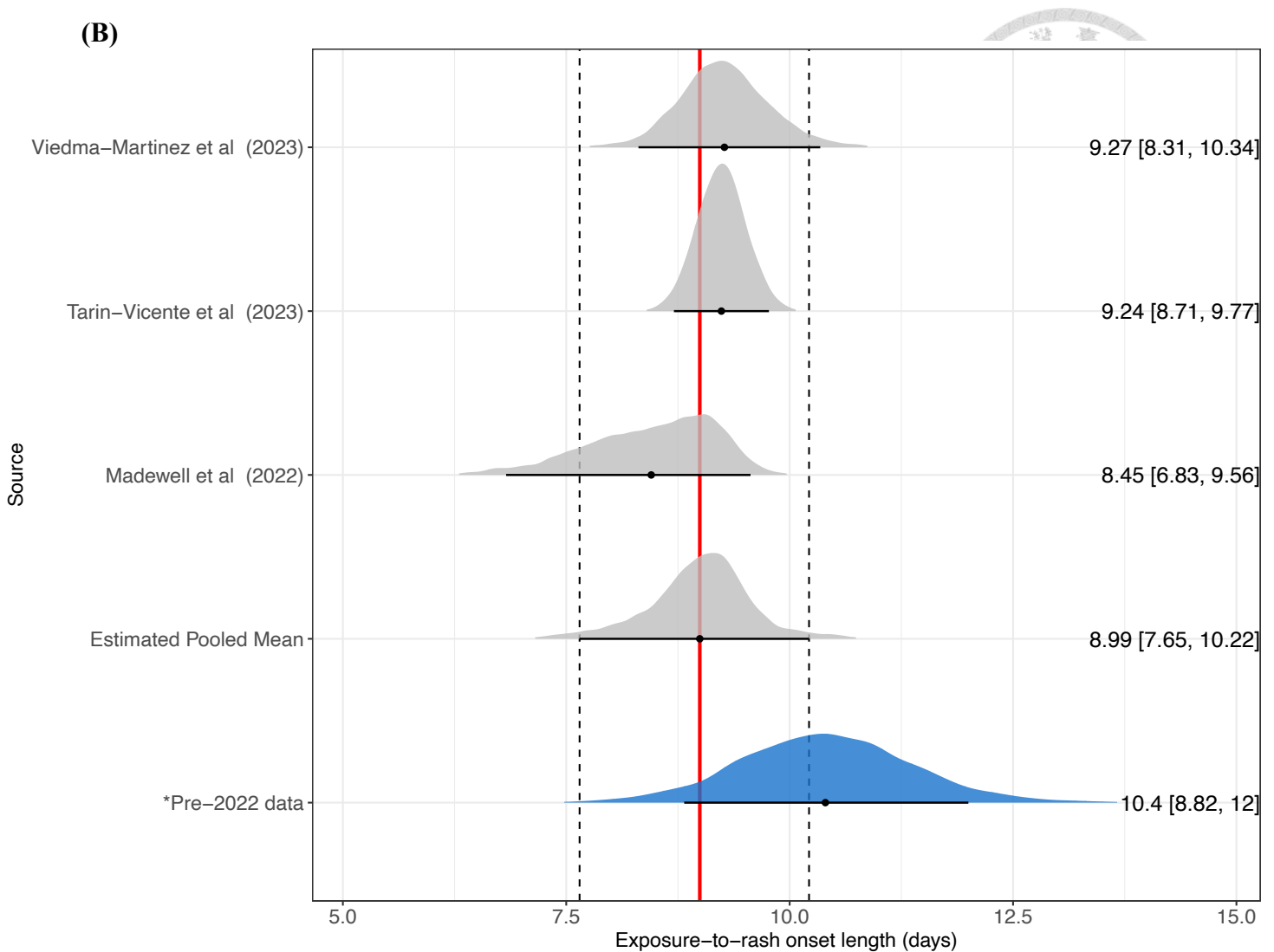
Fig. 6 Forest plot of the hierarchical/partial pooling meta-analysis model for the included **(A)** exposure-to-symptom onset period and **(B)** exposure-to-rash onset period estimates. Inclusion criteria involved the presence of an estimated mean estimate and standard deviation. The mean estimates displayed on the right represent the "partial pooling" model mean estimates and not the observed ones. *The blue density plots representing pre-2022 data were not used to derive the partially pooled mean estimates, but are plotted for comparison purposes.

Table 1

Exposure-to-symptom onset period estimates represented in Figure 4A
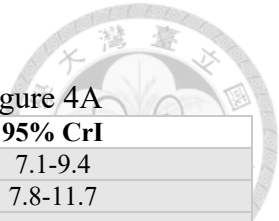
Source	Mean (days)	95% CrI
*Viedma-Martinez et al. (2023)	8.1	7.1-9.4
*Miura et al. (2022)	9.5	7.8-11.7
Guzzetta et al. (2022)	9.1	-
Madewell et al. (2022)	5.6	4.3-7.8
Ward et al. (2022)	7.8	6.6-9.2
Kroger et al. (2022)	8.2	-
*Tarin-Vicente et al. (2022)[R]	7.9	7.5-8.5
*Pre-2022 data	8.5	7.2-10.0
Thornhill et al. (2022)	7	-
Catalá et al. (2022)	6	-
Tarín-Vicente et al. (2022)	7	-
Mailhe et al. (2022)	6	-
Moschese et al. (2022)	11	-
Gomez-Garberi et al. (2022)	13	-
Angelo et al. (2022)	8	-
Besombes et al. (2022)	7	-
O'Laughlin et al. (2022)	7	-

Shaded rows represent the mean estimates while non-shaded rows represent the median estimates. Studies marked with an asterisk (*) represent mean exposure-to-symptom onset period estimates performed in this study. The highlighted study has not been peer-reviewed, but is included for comprehensive purposes. The superscript "R" represents that the data was adjusted for right truncation.

Table 2

Exposure-to-rash onset period estimates represented in Figure 4B

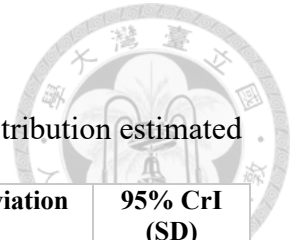| Source	Mean (days)	95% CrI
Viedma-Martinez et al. (2023)	9.7	8.3-11.2
Madewell et al. (2022)	7.6	6.3-9.3
Tarin-Vicente et al. (2022)	9.3	8.8-9.9
Pre-2022 data	10.6	8.8-12.8

Table 3

Observed exposure-to-symptom onset periods from each probability distribution estimated in this study

Dataset	Distribution	Mean (days)	95% CrI (mean)	Standard Deviation (days)	95% CrI (SD)
Pre-2022	Weibull	8.6	7.3-9.9	4.6	3.6-5.9
	Log-normal	**8.8**	**7.3-10.6**	**6.1**	**4.1-9.1**
	Gamma	8.5	7.2-10.0	4.8	3.6-6.3
Viedma-Martinez *et al.*	Weibull	8.1	6.9-9.3	3.3	2.7-4.2
	Log-normal	**8.1**	**7.1-9.4**	**3.2**	**2.2-4.7**
	Gamma	8.1	7.0-9.2	2.9	2.2-4.0
Miura *et al.*	Weibull	9.5	7.8-11.4	4.3	3.4-5.8
	Log-normal	**9.5**	**7.8-11.7**	**4.6**	**2.9-7.4**
	Gamma	9.3	7.7-11.1	4.0	2.8-5.8
Tarin-Vicente *et al.*	Weibull	7.9	7.5-8.4	3.3	3.0-3.7
	Log-normal	8.1	7.6-8.6	4.1	3.5-4.9
	Gamma	**7.9**	**7.5-8.5**	**3.5**	**3.1-4.0**

Table 4

Leave-one-out cross-validation information criterion estimates for IP models

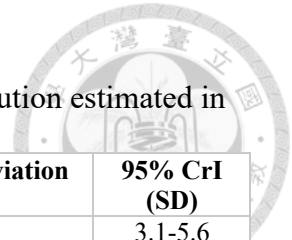| Dataset	Distribution	Deviance	Best-Fit Model
Pre-2022	Weibull	241.1	No significant difference
	Log-normal	242.6	
	Gamma	241.0	
Viedma-Martinez *et al.*	Weibull	106.9	Log-normal
	Log-normal	101.6	
	Gamma	102.5	
Miura *et al.*	Weibull	96.1	Log-normal
	Log-normal	91.7	
	Gamma	93.1	
Tarin-Vicente *et al.*	Weibull	737.0	Gamma
	Log-normal	743.8	
	Gamma	736.7	

Table 5

Observed exposure-to-rash onset periods from each probability distribution estimated in this study

Dataset	Distribution	Mean (days)	95% CrI (mean)	Standard Deviation (days)	95% CrI (SD)
Pre-2022	Weibull	10.4	8.8-12.0	4.1	3.1-5.6
	Log-normal	**10.6**	**8.8-12.8**	**5.3**	**3.4-8.4**
	Gamma	10.4	8.7-12.2	4.4	3.1-6.2
Viedma-Martinez *et al.*	Weibull	9.5	8.3-10.6	3.3	2.7-4.2
	Log-normal	**9.7**	**8.3-11.2**	**3.9**	**2.7-5.7**
	Gamma	9.5	8.3-10.8	3.4	2.5-4.5
Madewell *et al.*	Weibull	7.7	6.3-9.2	4.8	3.8-6.2
	Log-normal	**7.6**	**6.3-9.3**	**5.1**	**3.4-7.8**
	Gamma	7.5	6.3-9.0	4.5	3.4-6.1
Tarin-Vicente *et al.*	**Weibull**	**9.3**	**8.8-9.9**	**4.0**	**3.7-4.5**
	Log-normal	9.8	9.0-10.8	5.5	4.6-6.8
	Gamma	9.4	8.8-10.1	4.5	3.9-5.1

Table 6

Leave-one-out cross-validation information criterion estimates for exposure-to-rash onset models

Dataset	Distribution	Deviance	Best-Fit Model
Pre-2022	Weibull	134.9	No significant difference
	Log-normal	136.6	
	Gamma	135.0	
Viedma-Martinez *et al.*	Weibull	108.7	No significant difference
	Log-normal	109.6	
	Gamma	108.3	
Madewell *et al.*	Weibull	199.5	Log-normal
	Log-normal	190.5	
	Gamma	194.8	
Tarin-Vicente *et al.*	Weibull	792.6	Weibull
	Log-normal	803.5	
	Gamma	795.0	